1521-0103/381/2/68–78$35.00
THE JOURNAL OF PHARMACOLOGY AND EXPERIMENTAL THERAPEUTICS

dx.doi.org/10.1124/jpet.121.001076
J Pharmacol Exp Ther 381:68–78, May 2022

The Journal of PHARMACOLOGY And Experimental Therapeutics

Insulin Enhances Gene Expression of *Midnolin*, a Novel Genetic Risk Factor for Parkinson's Disease, via Extracellular Signal-Regulated Kinase, Phosphoinositide 3-Kinase and Multiple Transcription Factors in SH-SY5Y Cells[S]

Naoki Sagehashi, Yutaro Obara, Ohki Maruyama, Tadashi Nakagawa, Toru Hosoi, and Kuniaki Ishii

Department of Pharmacology, Yamagata University School of Medicine, Yamagata, Japan (N.S., Y.O., O.M., K.I.) and Department of Clinical Pharmacology, Faculty of Pharmaceutical Sciences, Sanyo-Onoda City University, Sanyo Onoda, Japan (T.N., T.H.)

Received December 27, 2021; accepted February 2, 2022

ABSTRACT

Parkinson's disease (PD) is the second most common neurodegenerative disease. Although many monogenic variants have been identified that cause familial PD, most cases are sporadic and the mechanisms of sporadic PD onset remain unclear. We previously identified *midnolin* (*MIDN*) as a novel genetic risk factor for PD in a Japanese population. *MIDN* copy number loss was strongly associated with sporadic PD, which was replicated in a British population. Furthermore, suppression of *MIDN* expression in rat pheochromocytoma cells inhibits neurite outgrowth and expression of Parkin ubiquitin ligase. However, the detailed molecular mechanisms of *MIDN* expression are unknown. We, therefore, investigated the molecular mechanism of *MIDN* expression in human neuroblastoma SH-SY5Y cells. We found that *MIDN* expression was promoted by insulin via extracellular-signal regulated kinase1/2 and phosphoinositide 3-kinase-dependent pathways. In addition, *MIDN* promoter activity was enhanced by mutations at transcription factor AP-2 consensus sequences and reduced by mutations at cAMP response element-binding protein and activator protein 1 (AP-1) consensus sequences. The dominant-negative cAMP response element-binding protein mutant did not block *MIDN* promoter activity, but both the pharmacological inhibitor and decoy oligodeoxynucleotide for AP-1 significantly blocked its activity. Additionally, DNA binding of c-FOS and c-JUN to the AP-1 consensus sequence in the *MIDN* promoter was enhanced by insulin as determined by chromatin immunoprecipitation, which suggested that AP-1 positively regulated *MIDN* expression. Taken together, this study reveals molecular mechanisms of *MIDN* gene expression induced by insulin in neuronal cells, and drugs which promote *MIDN* expression may have potential to be a novel medicine for PD.

SIGNIFICANCE STATEMENT

We demonstrated that insulin promotes *midnolin* expression via extracellular-signal regulated kinase 1/2 and phosphoinositide 3-kinase pathways. Furthermore, we identified the important region of the *MIDN* promoter and showed that transcription factors, including activator protein 1, positively regulate *MIDN* expression, whereas transcription factor AP-2 negatively regulates basal and insulin-induced *MIDN* expression. We believe that our observations are important and that they contribute to the development of novel drugs to treat Parkinson's disease.

Introduction

Parkinson's disease (PD) is the second most common neurodegenerative disease after Alzheimer's disease. PD prevalence increases with age, and it affects more than 1% of the population over the age of 60 (Lill, 2016). Typical symptoms include resting tremor, bradykinesia, rigidity, and postural instability, and loss of dopaminergic neurons projecting from the substantia nigra in the midbrain to the striatum is pathologically observed. Approximately 10% of PD cases are familial, and many monogenic variants and genetic risk factors have been identified, including *SNCA, PRKN, LRRK2,* and *GBA*

This work was supported in part by Grants-in-Aid from the Japan Society for the Promotion of Science [18K06681] (to Y.O.), Takeda Science Foundation (Y.O.), and Setsuro Fujii Memorial, the Osaka Foundation for Promotion of Fundamental Medical Research (Y.O.). The funding sponsors had no role in the design of the study, in the collection, analyses, or interpretation of the data, nor in the writing of the manuscript or the decision to publish the results.

The authors declare that they have no conflicts of interest with the contents of this article.

Material availability: There is a restriction to share the DNA plasmids (TFAP2 WT and mutants). Please contact Dr. Satoshi Maegawa (Shiga University of Medical Science, Japan) for permission to obtain the DNA plasmids.

dx.doi.org/10.1124/jpet.121.001076.

[S] This article has supplemental material available at jpet.aspetjournals.org.

ABBREVIATIONS: AP-1, activator protein 1; ATF, activating transcription factor; BDNF, brain-derived neurotrophic factor; ChIP, chromatin immunoprecipitation; CREB, cAMP response element-binding protein; ERK, extracellular-signal regulated kinase; GAPDH, glyceraldehyde-3-phosphate dehydrogenase; GIGYF2, Grb10-interacting GYF protein 2; MIDN, midnolin; NGF, nerve growth factor; ODN, oligodeoxynucleotide; PC12, pheochromocytoma; PD, Parkinson's disease; RT-qPCR, reverse transcription-quantitative polymerase chain reaction; TBST, Tris-buffered saline containing 0.1% tween-20; TFAP2, transcription factor AP-2.

(Lill, 2016; Scott et al., 2017; Billingsley et al., 2018; Smolders and Van Broeckhoven, 2020). The remaining cases are sporadic, and it is assumed that diverse genetic, epigenetic, and environmental factors interact in a complex manner to affect disease risk and progression; however, the mechanisms of sporadic PD onset remain unclear.

Midbrain nucleolar protein (midnolin or MIDN) was discovered in embryonic stem cells by a gene trap method in 2000 (Tsukahara et al., 2000). *Midn* was named after its specific expression pattern in the midbrain of embryonic (E)12.5 mouse embryos and the intracellular localization of MIDN in the nucleus and nucleolus. A ubiquitin-like domain and a nucleolar localizing sequence are adjacent to the amino and carboxy termini, respectively (Tsukahara et al., 2000). Although MIDN is abundant in the midbrain at early developmental stages, in the adult mouse it is also widely observed in other organs, including the heart, spleen, lungs, liver, skeletal muscles, kidneys, and testes (Tsukahara et al., 2000). The physiologic roles of MIDN were unclear for a long time, but in 2013, its ubiquitin-like domain was shown to interact with glucokinase (Hofmeister-Brix et al., 2013). MIDN inhibits glucokinase activity in vitro and glucose-induced insulin secretion from MIN6 cells. Meanwhile, exome analysis of Caucasian girls with autism spectrum disorder revealed many potential genetic variants, one of which was in *MIDN* (Butler et al., 2015), while array-based analyses showed duplications in 19p13.3, a region including *MIDN* and other genes that is associated with male infertility (Singh et al., 2019).

Molecular epidemiologic analyses show *MIDN* to be a novel genetic risk factor for sporadic PD. *MIDN* copy number loss (deletion) was significantly associated with sporadic PD in a Japanese cohort and this association was replicated in a large-scale British cohort (Obara et al., 2017; Obara et al., 2019). In Yamagata prefecture in northeast Japan, *MIDN* loss was observed in 10.5% of patients with sporadic PD whereas *MIDN* loss was not observed at all in healthy people. In Britain, *MIDN* loss was similarly observed in 6.55% of patients with sporadic PD and in 1.64% of a general population. This frequency (6.55–10.5%) is large compared with those of other causal variants, which are usually very small (<0.5%). In rat pheochromocytoma (PC12 cells), *MIDN* expression was enhanced by nerve growth factor (NGF). In addition, NGF-induced neurite outgrowth and expression of Parkin ubiquitin ligase were substantially inhibited by suppression of *MIDN* expression using genome-editing or RNA interference approaches (Obara et al., 2017; Obara and Ishii, 2018). Although typical DNA-binding or transcription-activating domains have not been identified in the MIDN protein, MIDN affects the transcription levels of a number of genes, including PD-related genes (Obara and Ishii, 2018), indicating that MIDN functions as a transcription modulator. Thus, we believe that *MIDN* loss is associated with PD although this is controversial (Billingsley et al., 2020; Obara et al., 2020).

MIDN expression in response to NGF is accompanied by the activation of extracellular signal-regulated kinase (ERK) 1/2 and ERK5 in PC12 cells (Obara et al., 2017). However, the detailed molecular mechanisms, particularly the *cis*-elements and transcription factors responsible for *MIDN* expression, are unknown. In this study, we therefore investigated the molecular mechanism of *MIDN* expression in human neuroblastoma SH-SY5Y cells.

Materials and Methods

Materials. Recombinant human insulin, all-trans retinoic acid, and wortmannin were purchased from Wako Pure Chemicals (Osaka, Japan). Brain-derived neurotrophic factor (BDNF) was purchased from Sigma-Aldrich (St. Louis, MO). Luciferin was purchased from AAT Bioquest (Sunnyvale, CA). SR11302 was purchased from Cayman Chemical (Ann Arbor, MI). U0126, primary antibodies against phospho-Akt (S473) (#9271), phospho-ERK1/2 (T202/Y204) (#9101), glyceraldehyde-3-phosphate dehydrogenase (GAPDH) (#3683), transcription factor AP-2β (TFAP2B) (#2509), phospho-cAMP response element-binding protein (CREB) (S133) (#9198), CREB (#9197) and c-FOS (#2250), and horseradish peroxidase-conjugated secondary antibody against rabbit IgG (#7074), were purchased from Cell Signaling Technology (Beverly, MA). Anti-ERK2 antibody (#sc-154) was purchased from Santa Cruz Biotechnology (Santa Cruz, CA). A synthetic double-stranded decoy oligodeoxynucleotide (ODN) was obtained from Fasmac (Atsugi, Japan). The decoy ODN was generated by annealing equimolar amounts of single-stranded sense and antisense phosphorothioate-modified ODNs that contained an AP-1-binding sequence (Moriyama et al., 2008). A scrambled double-stranded ODN was also generated and used as a control for the AP-1 decoy ODN. The phosphorothioate ODN used in this study was as follows: scrambled ODN (5′-TGT CTC TCT GAT GTC-3′ and 5′-GAC ATC AGA GAG ACA-3′) and decoy ODN for AP-1 (5′-TGT CTG ACT CAT GTC-3′ and 5′- GAC ATG AGT CAG ACA -3′) (AP-1 consensus sequences are underlined).

Cell Culture. Human neuroblastoma cells (SH-SY5Y cells) were kindly provided by Dr. Takeo Kato (Yamagata University, Japan) and grown in Dulbecco's modified Eagle's medium supplemented with 10% fetal bovine serum, penicillin (50 units/ml), and streptomycin (50 μg/ml) in a 5% CO_2 incubator at 37°C. Differentiation of the cells was induced by adding all-trans retinoic acid (10 μM) and incubating for 5 days as described above. For measurement of gene expression and protein phosphorylation levels, cells were incubated in serum-free medium before insulin and other drug stimulation.

DNA Constructs. The human *MIDN* promoter (−600 bp∼+125 bp) was amplified from genomic DNA of SH-SY5Y cells using a primer set (5′-CCC GCT AGC GCA TCC CCT CAC CAC ACT CCC-3′and 5′-CCC CTC GAG CCC CCT CCA CAC TCA CCG-3′) and PrimeStar MAX (Takara, Tokyo, Japan) and inserted between the NheI and XhoI sites of the pGL3-basic luciferase vector (Promega, Madison, WI). Deletion or variations were created by in vitro mutagenesis reactions using PrimeStar MAX. DNA plasmids encoding *TFAP2B* or its dominant-negative mutant (R225C) were kindly provided by Dr. Satoshi Maegawa (Shiga University of Medical Science, Japan) (Fuke et al., 2010). A plasmid encoding β-actin promoter-driven *β-galactosidase* was a kind gift from Dr. Philip Stork (Vollum Institute, Oregon Health Sciences University, OR). Plasmids that encoded *CREB* or its dominant-negative mutant (S133A) were a kind gift from Dr. Takeo Saneyoshi (Kyoto University, Japan).

Western Blotting. Cells were lysed in Laemmli buffer and proteins were separated on 11% polyacrylamide gels by electrophoresis. Then, the proteins were transferred to polyvinylidene difluoride membranes (GE Healthcare, Buckinghamshire, UK) using a semidry method. After blocking membranes with 5% skimmed milk, they were incubated with primary antibodies (1:1000 dilution). The membranes were washed three times and incubated with secondary antibody (1:5000 dilution). After rinsing the membranes, they were developed using an enhanced chemiluminescence kit (PerkinElmer, Waltham, MA or GE healthcare), and visualized with a ChemiDoc XRS imaging system (BioRad, Hercules, CA). The relative band intensities were analyzed using ImageJ densitometry software (National Institutes of Health, Bethesda, MD). The sample number for Western blotting was three for all cases. Quantitative data are shown in supplemental figures.

Luciferase Assay. SH-SY5Y cells were seeded into 24-well plates at 1×10^5 cells/well. Plasmids encoding the *MIDN* promoter linked to the firefly *luciferase* and β-actin-driven *β-galactosidase* genes, were cotransfected into cells using Lipofectamine 2000 (Invitrogen, Grand

Island, NY). After culture for 2 days, the cells were incubated in the presence or absence of insulin (1 μM) overnight. The cells were lysed and luciferase activity was measured using a GloMax20/20 luminometer (Promega) as described previously (Honda et al., 2015). As an internal control, β-actin promoter-driven β-galactosidase activity was measured to normalize for transfection efficiency as described previously (Honda et al., 2015).

Reverse Transcription-Quantitative Polymerase Chain Reaction (RT-qPCR). Total RNA from SH-SY5Y cells was extracted using TriPure isolation reagent (Roche, Indianapolis, IN) according to the manufacturer's protocol. The RNA was then reverse transcribed using an RT-PCR kit (Toyobo, Osaka, Japan), and real-time PCR was performed using FastStart Essential DNA Green Master for real-time PCR and a LightCycler Nano thermal cycler (Roche), as described previously (Kashino et al., 2018). The PCR primers used were as follows: *MIDN* (5′-GAG CAG ATG GAC TGC TCC CC-3′ and 5′-ACA AAG CTC TCG ATG ACG GC-3′), *c-FOS* (5′-CAG ACT ACG AGG CGT CAT CC-3′ and 5′-AGT TGG TCT GTC TCC GCT TG-3′), and *GAPDH* (5′-ACC ACA GTC CAT GCC ATC AC-3′ and 5′-TCC ACC ACC CTG TTG CTG TA-3′). PCR products were quantified and normalized to the *GAPDH* control before presentation as a fold change.

Chromatin Immunoprecipitation (ChIP) Analysis. ChIP assays were performed as described previously (Nakagawa et al., 2020) with some modifications. Briefly, ten million SH-SY5Y cells were fixed and centrifuged. The cell pellets were suspended in nuclear extraction buffer, and centrifuged again. The resulting pellets were suspended in Buf NUC solution, mixed with calcium chloride, and digested with micrococcal nuclease (New England Biolabs, M0247S). After the addition of 2 × sonication buffer to stop the reaction, the sample was centrifuged, and the supernatants were incubated with 6 μg of antibodies [IgG control (MBL, PM035), anti-c-JUN (Cell Signaling Technology, 9165) or anti-c-FOS (Cell Signaling Technology, 2250) antibody] conjugated to magnetic beads (Thermo Fisher, DB10004). Bead-bound proteins were washed with buffer A, buffer B, buffer C, and TE buffer, and the samples were then eluted by RNase A, proteinase K, and sodium chloride. After incubation with proteinase K again, DNA was purified with AMpure XP beads, eluted with TE buffer, and subjected to real-time PCR analysis with the use of Fast SYBR Green Master Mix (Thermo Fisher, 4385612). The primers for amplification of the *MIDN* promoter were 5′-TGG CTC GGG GCA TTC AAG-3′ and 5′-TTT ATC CGC GCC GCC TTC-3′ and those of *MIDN* intron 1 were 5′-CGG CTT TTC CCG GAC GAA-3′ and 5′-ACG GGT CTG GTA CCC CTC-3′.

Statistics. Data are expressed as the mean ± S.E.M, and the statistical significance of the differences was analyzed using Student's T-test (Fig. 8E) or one-way ANOVA with post hoc Tukey's test (Figs. 2C, 3A, 4A, 4B, 8A, 8C, and 8D; Supplemental Figs. 4, 5, 7, and 8) or Dunnett's test (Figs. 1A, 1B, 2A, 5B, 5C, 6A, and 7B; Supplemental Figs. 1, 2, 3, and 6) for multiple comparisons. StatView

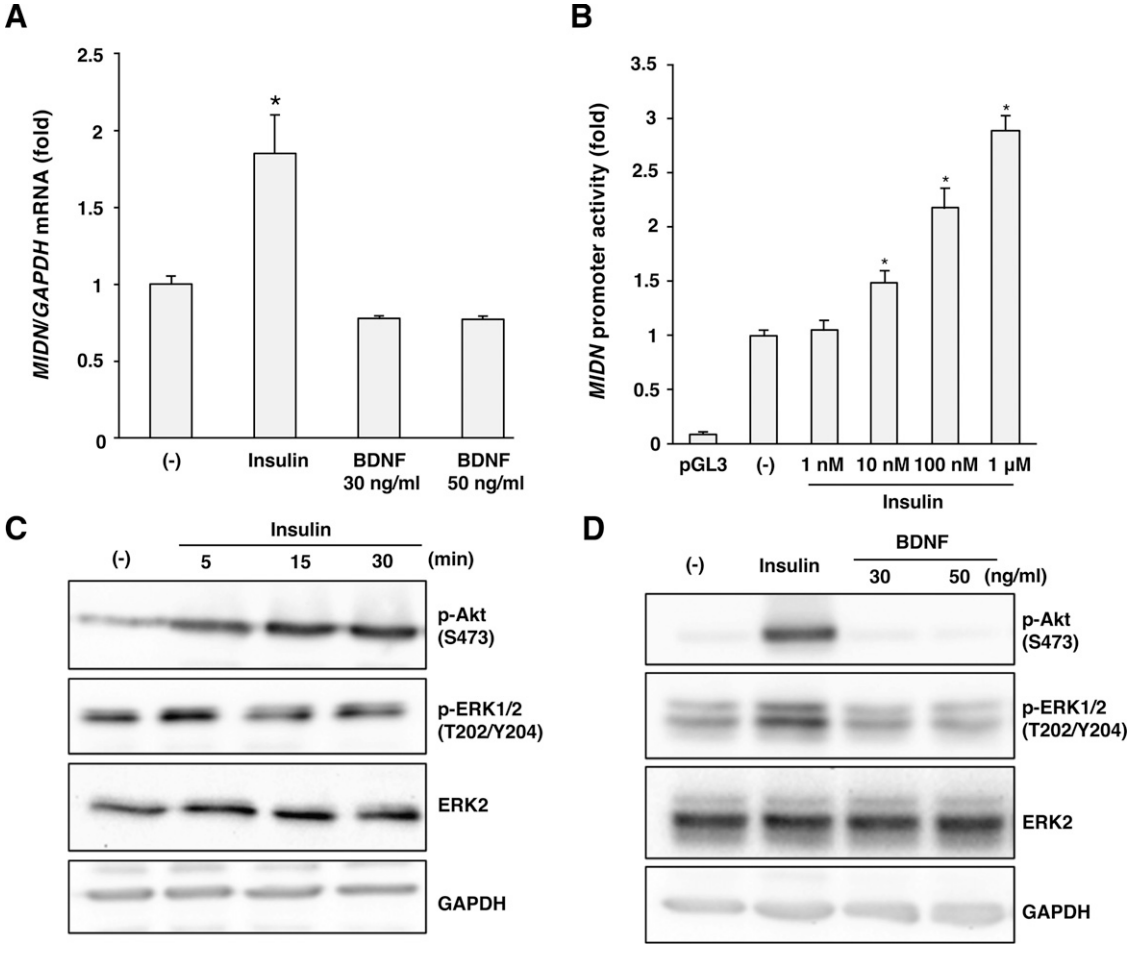

Fig. 1. Insulin promotes *MIDN* expression in SH-SY5Y cells. (A) SH-SY5Y cells were stimulated with insulin (1 μM) or BDNF (30 or 50 ng/ml) for 2 hours, then expression levels of *MIDN* were examined by RT-qPCR. Insulin significantly promoted *MIDN* expression (n = 3–9, $^*p < 0.05$). (B) SH-SY5Y cells were transfected with *MIDN* promoter (−600∼+125 bp) linked to *luciferase* in a promoterless plasmid (pGL3). After stimulation with insulin (1 nM to 1 μM), *MIDN* promoter activity was examined by measuring luciferase activity. Insulin significantly promoted *MIDN* promoter activity (n = 3, $^*p < 0.05$). (C) SH-SY5Y cells were stimulated with insulin (1 μM) for 5, 15, and 30 minutes, then phosphorylation of Akt and ERK1/2 was examined by Western blotting. (D) SH-SY5Y cells were stimulated with insulin (1 μM) or BDNF (30 or 50 ng/ml) for 5 minutes, then phosphorylation of Akt and ERK1/2 was examined by Western blotting.

software (ver5.0) (SAS institute Inc., Tokyo, Japan) was used for statistical analysis.

Results

Insulin Enhances MIDN Gene Expression in SH-SY5Y Cells. Human neuroblastoma SH-SY5Y cells were incubated with insulin (1 μM) or BDNF (30 or 50 ng/ml) for 2 hours, and *MIDN* expression levels were examined by RT-qPCR (Fig. 1A). *MIDN* expression was significantly enhanced by insulin, but not by BDNF. Next, we subcloned the human *MIDN* promoter region either side of the transcription start site (−600∼+125 bp) into pGL3, which encodes a promoterless firefly *luciferase*. In SH-SY5Y cells transfected with this DNA construct, the *luciferase* gene is efficiently expressed when the *MIDN* promoter is activated by a stimulant. We measured the human *MIDN* promoter activity in response to insulin (1 nM to 1 μM) and found it to be significantly increased in a concentration-dependent manner (Fig. 1B). To examine the signaling pathways activated by insulin, phosphorylation levels of ERK1/2 and Akt were examined as indices of activation of ERK1/2 and PI3-kinase, respectively. Insulin promoted phosphorylation of both ERK1/2 and Akt, but BDNF failed to cause the phosphorylation of Akt or ERK1/2 (Fig. 1, C and D and Supplemental Figs. 1 and 2). SH-SY5Y cells express the BDNF TrkB receptor and acquire sensitivity to BDNF during neuronal differentiation by retinoic acid (Sakane and Shidoji, 2011; Shiohira et al., 2012); therefore, the cells were incubated with retinoic acid (10 μM) for 5 days and were then stimulated with BDNF (50 ng/ml) or insulin (1 μM) for 1 or 2 hours. BDNF, in addition to insulin, significantly enhanced *MIDN* expression in these differentiated cells (Fig. 2A). BDNF (30 or 50 ng/ml) treatment of 5 minutes also caused phosphorylation of both ERK1/2 and Akt (Fig. 2B and Supplemental Fig. 3),

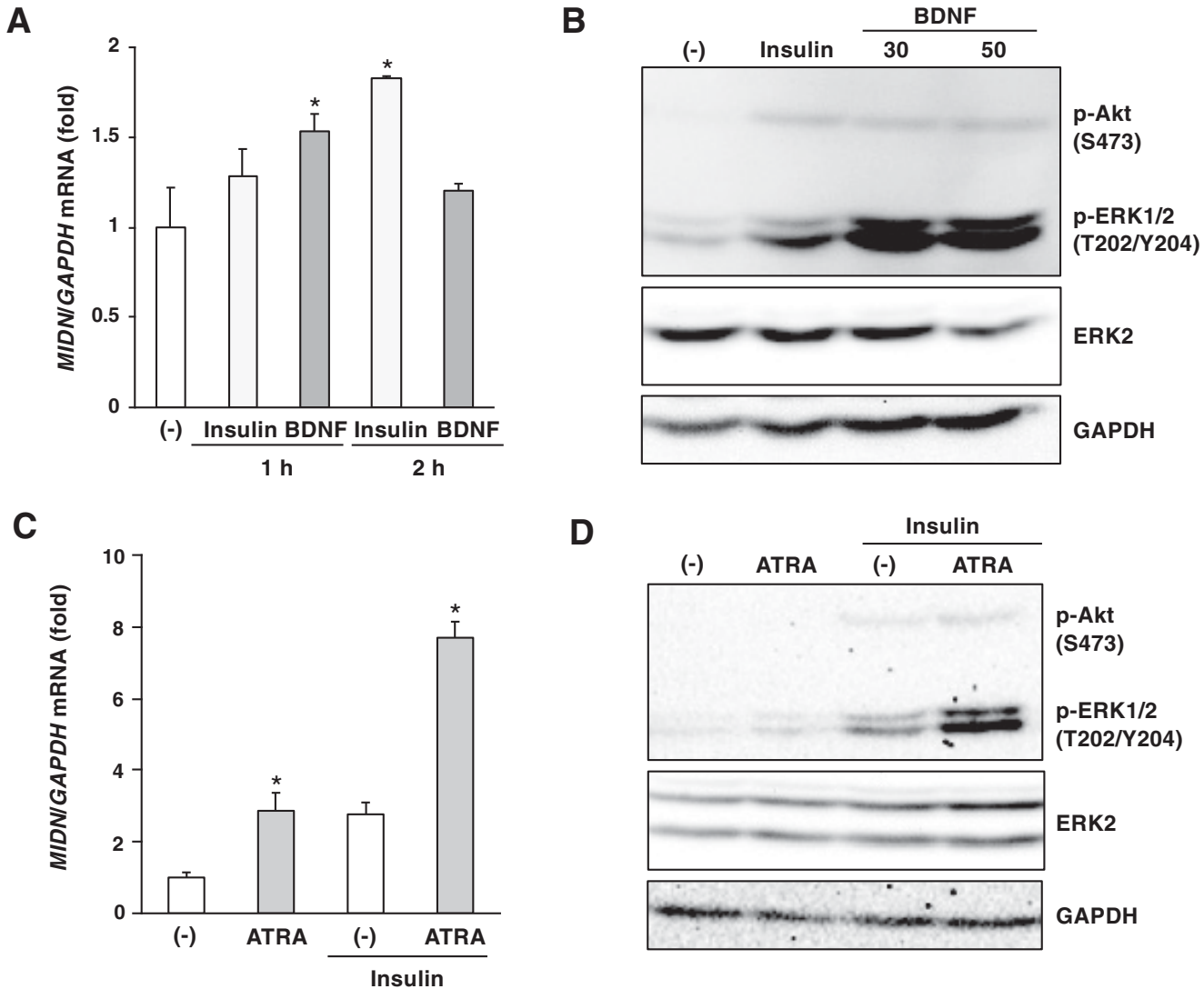

Fig. 2. BDNF and insulin promote *MIDN* expression in differentiated SH-SY5Y cells. (A) SH-SY5Y cells differentiated by all-trans retinoic acid (10 μM) for 5 days were stimulated with insulin (1 μM) or BDNF (50 ng/ml) for 1 or 2 hours, then expression levels of *MIDN* were examined by RT-qPCR. Insulin and BDNF significantly promoted *MIDN* expression (n = 3, *$p < 0.05$). (B) Differentiated SH-SY5Y cells were stimulated with insulin (1 μM) or BDNF (30 or 50 ng/ml) for 5 minutes, then phosphorylation of Akt and ERK1/2 was examined by Western blotting. (C) SH-SY5Y cells were incubated in the presence or absence of all-trans retinoic acid (10 μM) for 5 days and then stimulated with insulin (1 μM) for 2 hours. Then, expression levels of *MIDN* were examined by RT-qPCR. *MIDN* expression in differentiated cells was significantly higher than that in undifferentiated cells (n = 3, *$p < 0.05$). (D) Undifferentiated and differentiated SH-SY5Y cells were stimulated with insulin (1 μM) for 5 minutes and then phosphorylation of Akt and ERK1/2 was examined by Western blotting.

confirming that the TrkB receptor tyrosine kinase was activated by BDNF in the differentiated cells. When *MIDN* expression was compared between undifferentiated and differentiated cells under the same conditions, *MIDN* expression in differentiated cells was significantly higher than that in undifferentiated cells, although insulin increased *MIDN* expression levels to a similar extent regardless of differentiation states (Fig. 2C). Phosphorylation of ERK1/2 and Akt was related to *MIDN* expression levels (Fig. 2D and Supplemental Fig. 4). However, because the effect of insulin was more potent than that of BDNF and obvious in both undifferentiated and differentiated cells, we focused on insulin signaling that led to *MIDN* expression in undifferentiated cells. SH-SY5Y cells were preincubated in the presence or absence of a MEK inhibitor, U0126 (30 μM), or a PI3-kinase inhibitor, wortmannin (500 nM), for 30 minutes, then stimulated with insulin (1 μM) for 2 hours. RT-qPCR analysis showed that insulin increased *MIDN* expression, which was largely blocked by U0126 or wortmannin and was completely suppressed by the combination of U0126 and wortmannin (Fig. 3A). Inhibition of PI3-kinase and ERK1/2 by these inhibitors was confirmed by Western blotting (Fig. 3B and Supplemental Fig. 5). These data indicate that insulin promotes *MIDN* expression accompanied by the activation of ERK1/2 and PI3-kinase in SH-SY5Y cells.

Transcription Factors, Including TFAP2 and AP-1, Regulate Human MIDN Promoter Activity in SH-SY5Y Cells. To examine the insulin signaling pathway involved in increased *MIDN* expression in more detail, we measured *MIDN* promoter activity using reporter plasmids encoding various length of the *MIDN* promoter (−600, −450, −300, −150, −100, and −50 bp to +125 bp). We found a region that negatively regulates promoter activity between −150 bp and −100 bp and a region that positively regulates its activity between −100 and −50 bp (Fig. 4A). This was also observed after insulin stimulation (Fig. 4B), suggesting that multiple transcription factors are involved in *MIDN* expression.

In silico analysis of the JASPAR2020 database (Fornes et al., 2020) identified TFAP2 consensus sequences between −121 bp and −99 bp upstream of the transcription start site (5′-AGC CGT CAA GGC GCC CCA GGG CC-3′). The highest TFAP2 family member binding affinity scores were 12.9646 for TFAP2A, 12.2031 for TFAP2B and 12.6803 for TFAP2C, indicating that the sequence in this region of the *MIDN* promoter is highly similar to the consensus sequence for all TFAP2 isoforms (Supplemental Table 1). We also discovered the consensus sequence for activator protein 1 (AP-1) and for the CREB/Activating transcription factor (ATF) family in the promoter region between −71 bp and −57 bp (5′-GTC TGC GTC ACC GCC-3′) (Supplemental Tables 2–4). The highest scores for binding affinity with these transcription factors were 10.5189 for FOSL1/JUN, 10.9754 for ATF1 and 11.1485 for CREB1. Furthermore, there is a region between these sites putatively recognized by various other transcription factors including KLF, SP, and EGR family members. To identify the specific *cis*-elements involved in *MIDN* expression, the putative binding sequences for these transcription factors were mutated as indicated in Fig. 5A. Both basal and insulin (1 μM)-stimulated *MIDN* promoter activity was significantly enhanced by mutations at TFAP2 consensus sites (Mut 1 and 2) and also by mutations 3 and 4 (Fig. 5B). In contrast, basal and insulin (1 μM)-stimulated *MIDN* promoter activity was significantly reduced by the mutation at the CREB/ATF family and AP-1 family consensus sites (Mut 5) (Fig. 5C).

Because TFAP2 was suggested to be involved in regulation of *MIDN* expression, wild-type TFAP2B and its dominant-

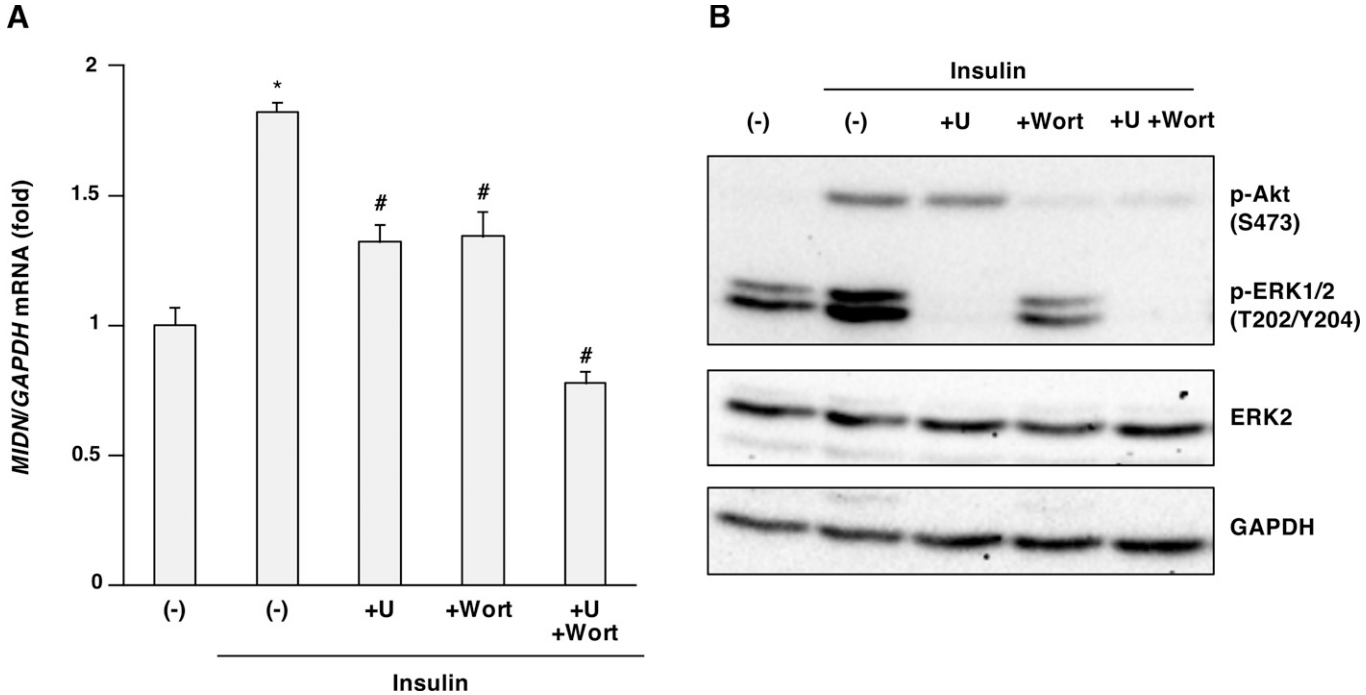

Fig. 3. Insulin promotes *MIDN* expression via PI3-kinase and ERK1/2 in SH-SY5Y cells. (A) SH-SY5Y cells were preincubated with or without U0126 (U, 30 μM) or wortmannin (Wort, 500 nM) for 30 minutes, then stimulated with insulin (1 μM) for 2 hours. Expression levels of *MIDN* were examined by RT-qPCR. Insulin significantly promoted *MIDN* expression ($^*p < 0.05$), which was significantly blocked by U0126 and wortmannin (n = 3–6, $^{\#}p < 0.05$). (B) SH-SY5Y cells were preincubated with or without U0126 (U, 30 μM) or wortmannin (Wort, 500 nM) for 30 minutes, then stimulated with insulin (1 μM) for 2 hours. Phosphorylation of Akt and ERK1/2 was examined by Western blotting.

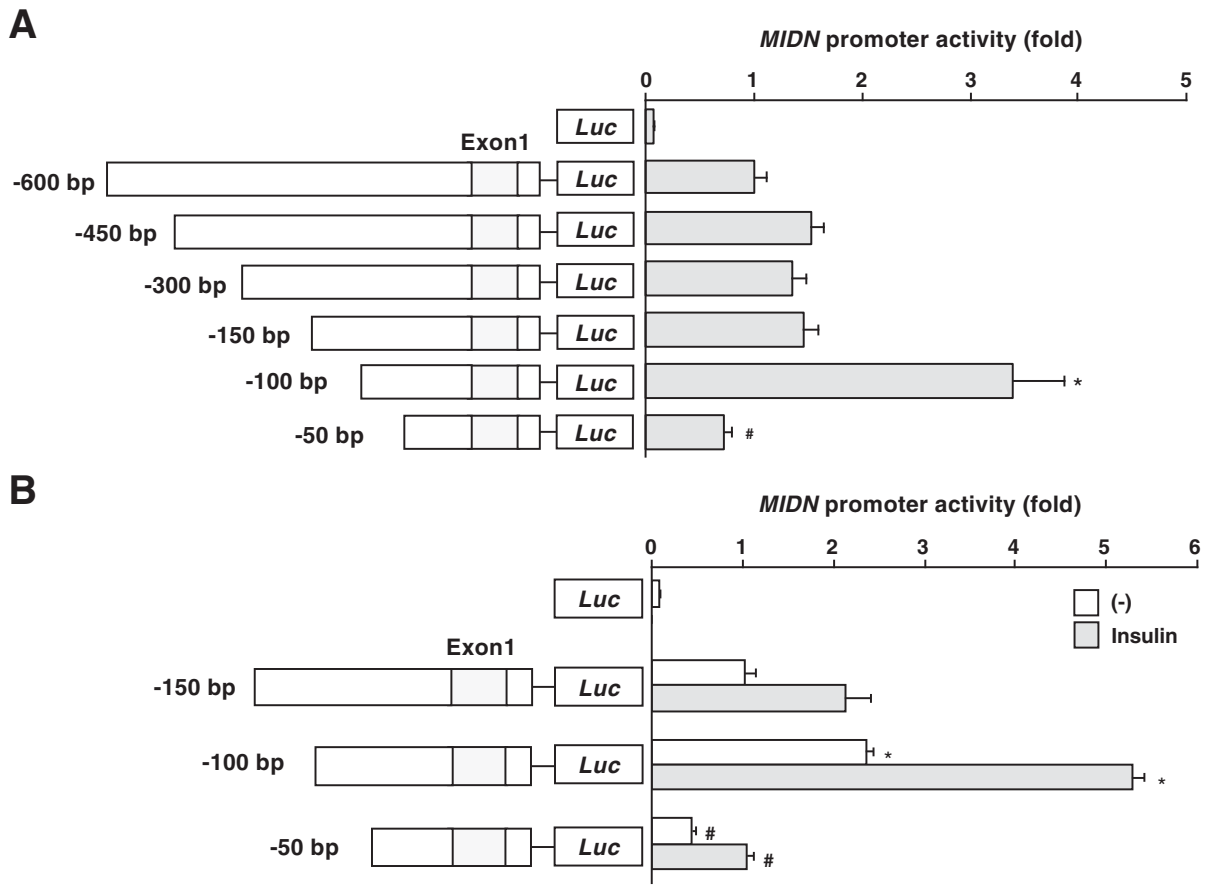

Fig. 4. Insulin regulates *MIDN* promoter activity between −150 and −50 bp upstream of the transcription start site. (A) SH-SY5Y cells were transfected with different length *MIDN* promoters (−600, −450, −300, −150, −100, or −50 to +125 bp) linked to *luciferase* in a promoterless plasmid (pGL3) and *MIDN* promoter activity was examined by measuring luciferase activity. *MIDN* promoter activity of the −100∼+125 bp fragment was significantly enhanced compared with that of the −150∼+125 bp fragment ($n = 6$, $^{*}p < 0.05$). The activity of the −50∼+125 bp fragment was significantly reduced compared with that of the −100∼+125 bp fragment ($n = 6$, $^{\#}p < 0.05$). (B) SH-SY5Y cells were transfected with different length *MIDN* promoters (−150, −100, or −50 to +125 bp) linked to *luciferase* in a promoterless plasmid (pGL3) and stimulated with insulin (1 μM). *MIDN* promoter activity was examined by measuring luciferase activity. *MIDN* promoter activity of the −100∼+125 bp fragment was significantly enhanced compared with that of the −150∼+125 bp fragment ($n = 3$, $^{*}p < 0.05$) and the activity of the −50∼+125 bp fragment was significantly reduced compared with that of the −100∼+125 bp fragment ($n = 3$, $^{\#}p < 0.05$) in both the presence and absence of insulin.

negative mutant (R225C) were overexpressed in SH-SY5Y cells and *MIDN* promoter activity (−150∼+125) was measured. This dominant-negative mutant lacks DNA-binding ability (Fuke et al., 2010). Although overexpression of TFAP2 did not reduce the promoter activity, its dominant-negative mutant promoted promoter activity (Fig. 6A), indicating that TFAP2B negatively regulates *MIDN* expression. Overexpression of TFAP2B and TFAP2B R225C was confirmed by Western blotting (Fig. 6B and Supplemental Fig. 6).

To investigate the activity and involvement of CREB in *MIDN* expression, phosphorylation levels of CREB and ATF1 were also examined by Western blotting as an index of activation. The phospho-specific CREB antibody used also recognizes phospho-ATF1 (S63), but only phosphorylation of CREB was enhanced by insulin (1 μM); there was no conclusive phosphorylated ATF1 band (Fig. 7A). Densitometric analysis showed that U0126 (30 μM) blocked this CREB phosphorylation by 50.0% ($n = 3$, $p < 0.05$), while wortmannin (500 nM) only reduced it by 17.3% ($n = 3$, $p > 0.05$), indicating that insulin activates CREB, which was accompanied mainly by ERK1/2 signaling (Supplemental Fig. 7). Additionally, a dominant-negative mutant of CREB S133A, which lacked its phosphorylation sites at Ser133, was overexpressed in cells stimulated with insulin (1 μM). However, the *MIDN* promoter was not inhibited by the CREB S133A mutant (Fig. 7B).

Next, to investigate the activity and involvement of AP-1 in *MIDN* expression, mRNA and protein expression levels of c-FOS were measured by RT-qPCR and Western blotting, respectively, as an index of AP-1 transcriptional activity. Insulin (1 μM) significantly enhanced *c-FOS* mRNA expression, which was significantly reversed by U0126 (30 μM), but not wortmannin (500 nM), which suggested that the ERK1/2 pathway was involved in *c-FOS* induction (Fig. 8A). c-FOS protein was also induced by insulin treatment (1 μM) for 2 hours, which was completely inhibited by U0126 (30 μM) and partially, but significantly, inhibited by wortmannin (500 nM) (Fig. 8B and Supplemental Fig. 8). To examine the involvement of AP-1 in *MIDN* expression, the decoy ODN (2 μg/well) for AP-1 was cotransfected with reporter genes into cells that were stimulated with insulin (1 μM). As a result, the decoy ODN for AP-1 completely inhibited the insulin (1 μM)-induced *MIDN* promoter activation (Fig. 8C). To confirm the roles of AP-1, we used a pharmacological inhibitor, SR11302, which is a synthetic retinoid derivative that inhibits AP-1 activity without

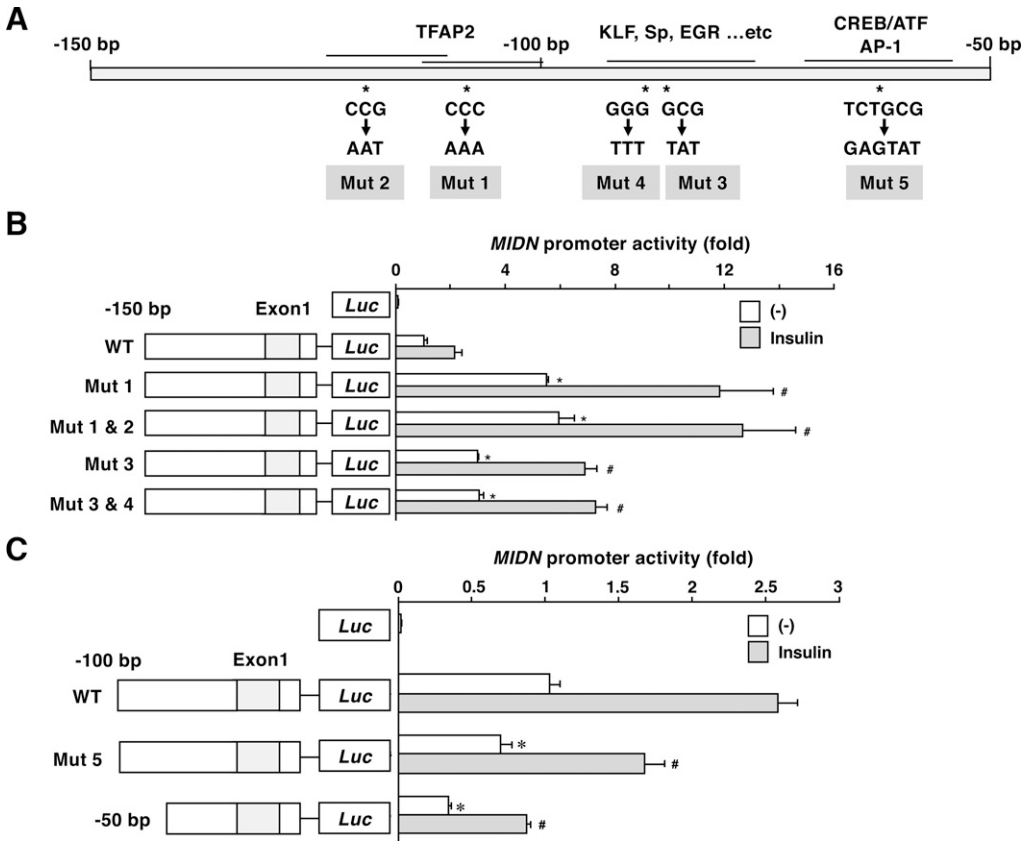

Fig. 5. cis-elements for TFAP2, AP-1 and CREB/ATF are involved in basal and insulin-induced *MIDN* expression. (A) Depiction of mutated sites in the *MIDN* promoter between −150 and −50 bp. Putative binding sequences for various transcription factors were mutated as indicated (Mut 1–5). (B) SH-SY5Y cells were transfected with wild-type or mutated (Mut 1–4) *MIDN* promoter (−150∼+125 bp) linked to *luciferase* in a promoterless plasmid (pGL3), and stimulated with insulin (1 μM). *MIDN* promoter activity was examined by measuring luciferase activity. The mutated *MIDN* promoter activity was significantly enhanced compared with the wild-type promoter activity in both the presence and absence of insulin (n = 3, $^{*,\ \#}p < 0.05$). (C) SH-SY5Y cells were transfected with wild-type or mutated (Mut 5) *MIDN* promoter (−100 or −50∼+125 bp) linked to *luciferase* in a promoterless plasmid (pGL3), and stimulated with insulin (1 μM). *MIDN* promoter activity was examined by measuring luciferase activity. The activity of *MIDN* promoter (Mut 5 and −50∼+125 bp) was significantly reduced compared with the wild-type promoter activity (−100∼+125 bp) in both the presence and absence of insulin (n = 6, $^{*,\ \#}p < 0.05$).

activating retinoid response elements (Li et al., 1997). SR11302 (30 μM) significantly inhibited the *MIDN* promoter activation induced by insulin (Fig. 8D). Finally, a ChIP assay was performed using c-FOS and c-JUN antibodies to confirm that AP-1 bound to its consensus sequence (−71 to −57 bp) in the *MIDN* promoter and identify the AP-1 isoforms involved in this case (Fig. 8E). As expected, insulin (1 μM) significantly promoted DNA binding of both c-FOS and c-JUN to its predicted corresponding sequence, but not to intron 1 (+840 to +969 bp) as a negative control sequence. Taken together, these results suggest that AP-1 rather than CREB is involved in insulin-induced *MIDN* expression, although CREB is also activated by insulin in an ERK1/2-dependent manner.

Discussion

In this study, we found that insulin promoted *MIDN* expression in human neuroblastoma cells via ERK1/2 and PI3-kinase-dependent pathways. In addition, the *MIDN* promoter was regulated in multiple ways by various transcription factors. AP-1 enhances, whereas TFAP2 suppresses, *MIDN* expression. These signaling pathways are depicted in Fig. 9.

Although insulin generally modulates peripheral glucose metabolism, it is efficiently transported into the brain through its specific mechanism to cross the blood brain barrier (Ghasemi et al., 2013; Gray and Barrett, 2018). Insulin transcripts have been detected in GABAergic neurogliaform cells in the cortex, which act in cortical microcircuits (Molnar et al., 2014), and in the rat hippocampus (Nemoto et al., 2014). Furthermore, insulin-like growth factor 1/2, which interacts with insulin receptors, is biosynthesized in glial cells. Insulin receptor is abundantly expressed in the central nervous system, especially in postsynaptic neurons (Wada et al., 2005), which suggests that central insulin regulates behavior and cognitive functions other than glucose homeostasis (Zhao and Alkon, 2001). Moreover, dysfunction in insulin signaling is associated with neurodegenerative diseases (Moroo et al., 1994; Craft and Watson, 2004; Trejo et al., 2004). Remarkably, Grb10-interacting GYF protein 2 (GIGYF2) interacts with insulin and insulin-like growth factor receptors through Grb10, and mutations in the *GIGYF2* gene within the *Park11* locus have been associated with PD (Lautier et al., 2008; Blauwendraat et al., 2020). *Gigyf2* knockout mice exhibit motor dysfunction and α-synuclein-positive plaques, which implies that abnormal insulin signaling is associated with PD (Giovannone et al., 2009).

Although the relationship between PD and diabetes mellitus has been controversial, the shared biologic mechanisms and positive clinical and epidemiologic association between type 2

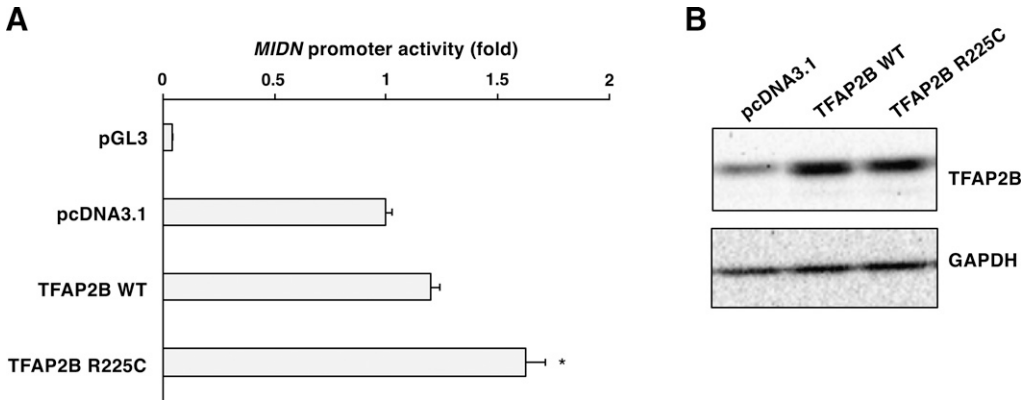

Fig. 6. A dominant-negative TFAP2B mutant enhanced *MIDN* promoter activity in SH-SY5Y cells. (A) SH-SY5Y cells were cotransfected with wild-type *MIDN* promoter (−150∼+125 bp) linked to *luciferase* in a promoterless plasmid (pGL3) and empty vector (pcDNA3.1), wild-type TFAP2B (WT) or a dominant-negative TFAP2B mutant (R225C). *MIDN* promoter activity was examined by measuring luciferase activity. *MIDN* promoter activity was significantly enhanced by overexpression of TFAP2B R225C ($n = 6$, $^{*}p < 0.05$). (B) SH-SY5Y cells were cotransfected with reporter plasmids and TFAP2B WT or its dominant-negative mutant as described above, and overexpression of TFAP2B and TFAP2B-R225C was examined by Western blotting.

diabetes and PD are currently an interesting hypothesis (Sánchez-Gómez et al., 2020; 2021). Whereas certain oral antidiabetic drugs, which include pioglitazone and metformin, have not had a significant benefit in clinical trials, daily intranasal administration of insulin improved motor impairment and had a positive effect on cognitive functions (Novak et al., 2019). Furthermore, exenatide, an agonist of the glucagon-like peptide-1 receptor, exerted a positive effect on practically defined off-medication motor scores in a clinical trial for PD patients, although the effect of exenatide on pathophysiology and long-lasting symptomatic improvement remains unclear (Athauda et al., 2017; 2019). The relevance of PD to diabetes and the effectiveness of antidiabetic drugs on PD should be clarified in both in vitro and in vivo/clinical studies.

We previously showed that *MIDN* expression was enhanced by NGF, but not by epidermal growth factor or basic fibroblast growth factor in PC12 cells (Obara et al., 2017). In addition, the NGF-induced *MIDN* expression was both ERK1/2 and ERK5-dependent. In this study, insulin enhanced *MIDN* expression in SH-SY5Y cells accompanied by activation of ERK1/2 and PI3-kinase (Figs. 1 and 3). *MIDN* expression was also enhanced by BDNF in cells differentiated by retinoic acid and in which TrkB receptor was induced (Sakane and Shidoji, 2011; Shiohira et al., 2012) (Fig. 2). The majority of neurotrophic factors and growth factors activate both ERKs and PI3-kinase in a similar manner through their specific receptor tyrosine kinases. However, there are differences in the intracellular signaling that depend on the growth factors and cell type. For example, NGF causes sustained ERK1/2 activation via the small G-proteins, Ras and Rap1, whereas this activation is only transient and Ras-dependent in case of epidermal growth factor in PC12 cells (York et al., 1998; Obara et al.,

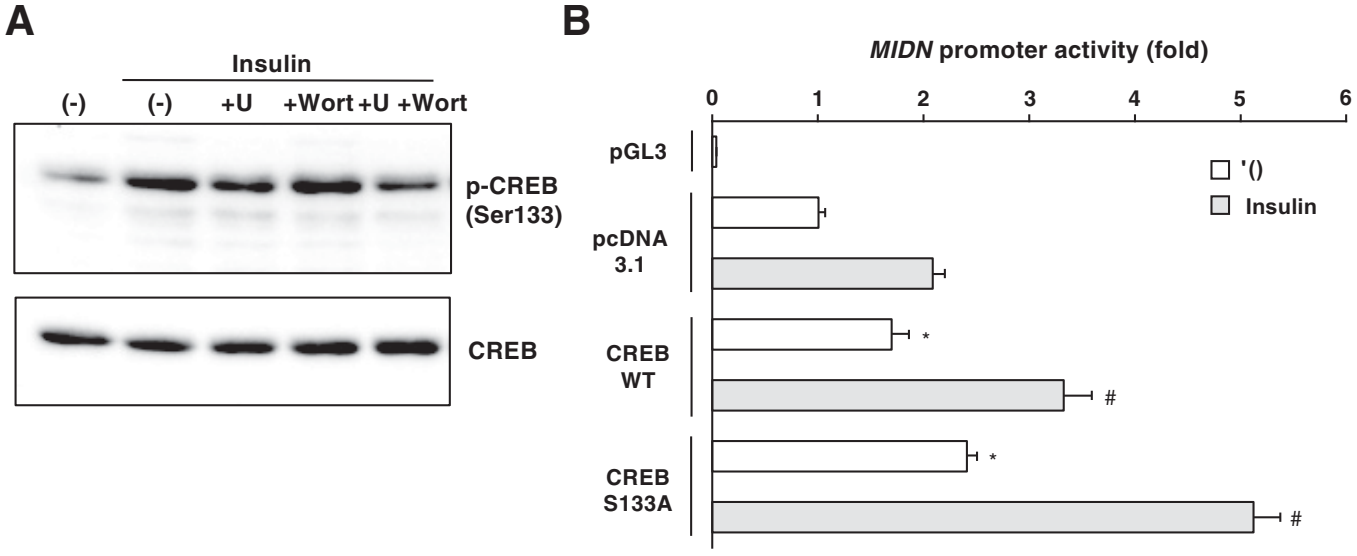

Fig. 7. CREB is not involved in *MIDN* promoter activation by insulin in SH-SY5Y cells. (A) SH-SY5Y cells were preincubated in the presence or absence of U0126 (U, 30 μM) or wortmannin (Wort, 500 nM) for 30 minutes and then stimulated with insulin (1 μM) for 2 hours. Phosphorylation of CREB was examined by Western blotting. (B) SH-SY5Y cells were cotransfected with wildtype *MIDN* promoter (−100∼+125 bp) linked to *luciferase* in a promoterless plasmid (pGL3) and empty vector (pcDNA3.1), wildtype CREB (WT) or a dominant-negative CREB mutant (S133A) and then stimulated with insulin (1 μM). *MIDN* promoter activity was examined by measuring luciferase activity. *MIDN* promoter activity was significantly enhanced by overexpression of CREB WT and the S133A mutant ($n = 3$, $^{*,\#}p < 0.05$).

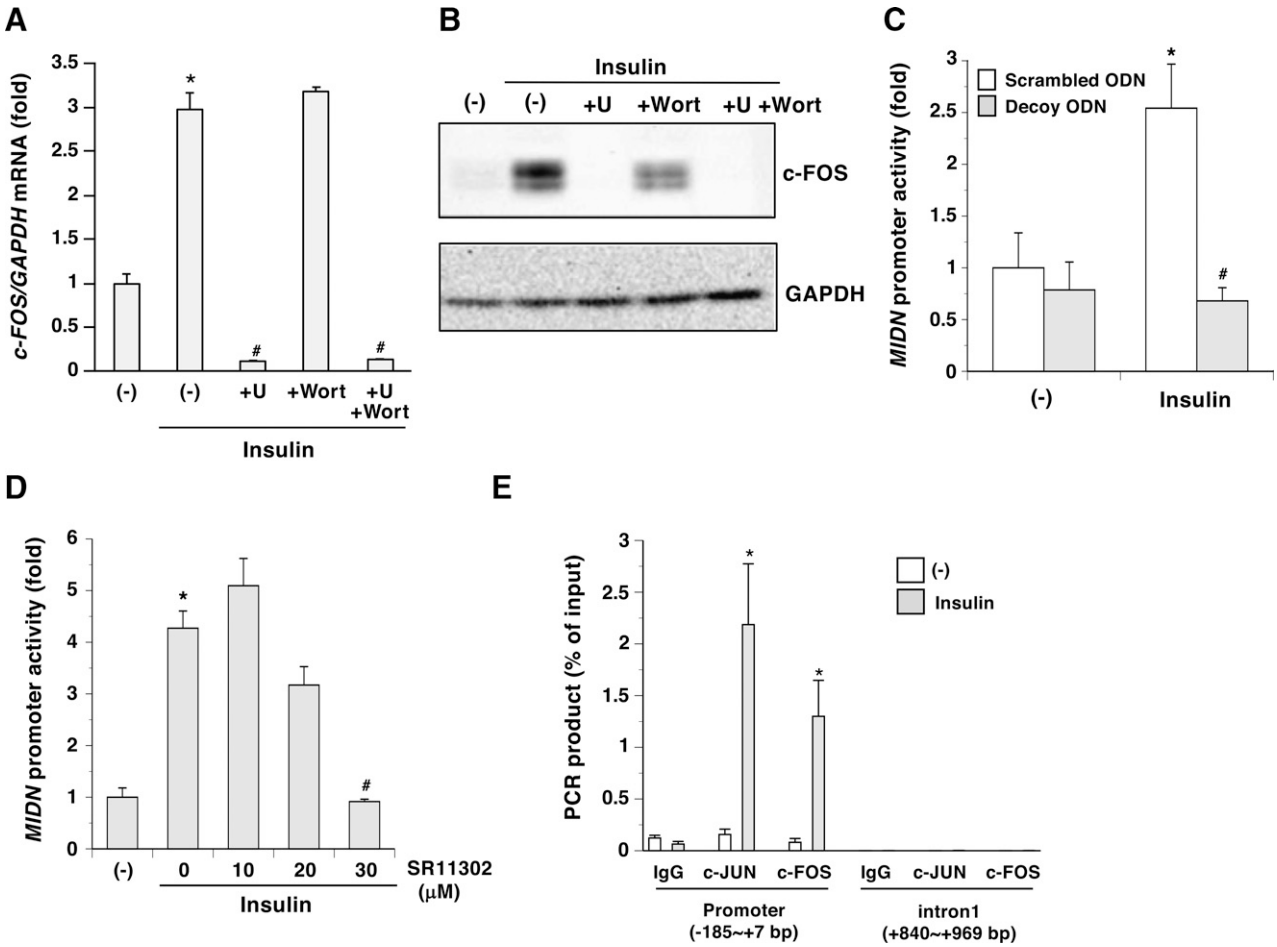

Fig. 8. Insulin promotes *c-FOS* expression and AP-1 is involved in *MIDN* promoter activation by insulin in SH-SY5Y cells. (A) SH-SY5Y cells were preincubated in the presence or absence of U0126 (U, 30 μM) or wortmannin (Wort, 500 nM) for 30 minutes, then stimulated with insulin (1 μM) for 2 hours. Gene expression levels of *c-FOS* were examined by RT-qPCR. Insulin significantly promoted *c-FOS* expression (n = 3–6, $^{*}p < 0.05$), which was significantly blocked by U0126 (n = 3–6, $^{\#}p < 0.05$). (B) SH-SY5Y cells were preincubated in the presence or absence of U0126 (U, 30 μM) or wortmannin (Wort, 500 nM) for 30 minutes, then stimulated with insulin (1 μM) for 2 hours. c-FOS and GAPDH levels were examined by Western blotting. (C) SH-SY5Y cells were cotransfected with wildtype *MIDN* promoter (−100∼+125 bp) linked to *luciferase* in a promoterless plasmid (pGL3) and scrambled or decoy ODNs (2 μg) and then stimulated with insulin (1 μM). *MIDN* promoter activity was examined by measuring luciferase activity. Insulin significantly promoted *MIDN* promoter activity (n = 6, $^{*}p < 0.05$), which was significantly blocked by the decoy ODN (n = 6, $^{\#}p < 0.05$). (D) SH-SY5Y cells were transfected with the wildtype *MIDN* promoter (−100∼+125 bp) linked to *luciferase* in a promoterless plasmid (pGL3). The cells were preincubated with or without SR11302 (10–30 μM) and then stimulated with insulin (1 μM). *MIDN* promoter activity was examined by measuring luciferase activity. Insulin significantly promoted *MIDN* promoter activity (n = 4–8, $^{*}p < 0.05$), which was significantly blocked by SR11302 (n = 4–8, $^{\#}p < 0.05$). (E) SH-SY5Y cells were stimulated with insulin (1 μM) for 2 hours. Then, ChIP assays were performed using control IgG, c-JUN, and c-FOS antibodies. The *MIDN* promoter region (−185 to +7 bp), which included the predicted AP-1 consensus sequence (−71 to −57 bp), and intron 1 (+840 to +969 bp) was amplified by qPCR. Insulin significantly promoted DNA binding of both c-JUN and c-FOS to the *MIDN* promoter region (n = 3, $^{*}p < 0.05$).

2004). This difference affects cell fate; NGF induces neuronal differentiation and epidermal growth factor promotes proliferation. The reason why only certain neurotrophic factors or growth factors affect *MIDN* expression remains unknown, but it is suggested that NGF or insulin-specific signaling pathways in addition to those involving ERKs and PI3-kinase may be responsible for *MIDN* expression. Because growth/neurotrophic factors, including insulin, BDNF and glial cell-derived neurotrophic factor, have neurotrophic effects and clinical potential for the treatment of PD (Allen et al., 2013; Shaughness et al., 2020), it is important to examine whether they induce *MIDN* expression, particularly in vivo.

By *MIDN* promoter analysis, we found that TFAP2 negatively regulated *MIDN* expression. Deleting or mutating the TFAP2 consensus sequence between −121 bp and −99 bp upstream of the transcription start site (5′-AGC CGT CAA GGC GCC CCA GGG CC-3′) increased promoter activity (Figs. 4 and 5; Supplemental Table 1). In addition, the promoter activity was promoted by overexpression of a dominant-negative TFAP2B mutant that lacks DNA binding activity (Fig. 6A). However, overexpression of wild-type TFAP2B did not cause a significant reduction of promoter activity. SH-SY5Y cells express TFAP2B (Fig. 6B), which may be sufficient for negative regulation of the *MIDN* promoter. Generally, TFAP2 forms homo- or hetero-dimers with other TFAP2 family members, and functions as both an activator and repressor of gene transcription. TFAP2B mediates retinoic acid-induced noradrenergic neuronal differentiation in neuroblastoma, including SH-SY5Y cells (Ikram et al., 2016). In our study, TFAP2 suppressed *MIDN* gene expression in SH-SY5Y cells, but the physiologic significance of this remains unknown. It is necessary to clarify the molecular mechanism by which insulin regulates

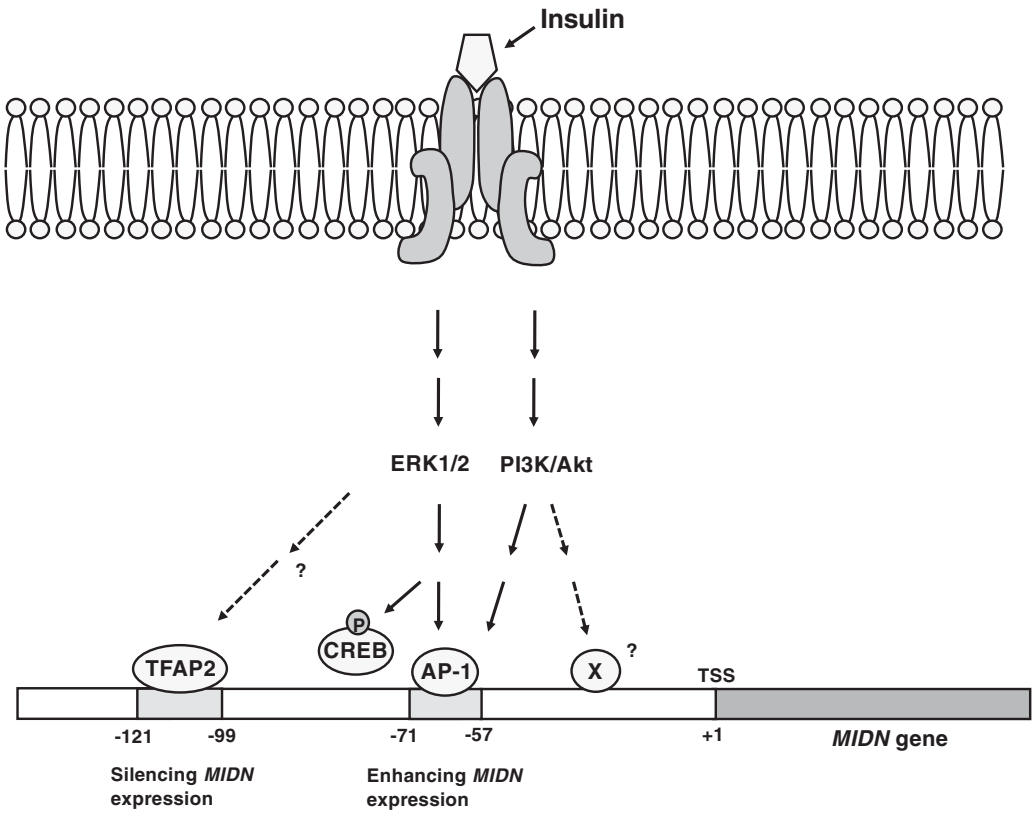

Fig. 9. A putative insulin signaling pathway for promoting *MIDN* expression. Insulin upregulates *MIDN* expression accompanied by the activation of ERK1/2 and PI3-kinase pathways. It is assumed that AP-1 rather than CREB promotes *MIDN* expression downstream of ERK1/2 and PI3-kinase pathways, whereas TFAP2 suppresses *MIDN* expression.

TFAP2 activity and how TFAP2 inhibits *MIDN* expression. We discovered that the promoter region between −71 bp and −57 bp (5′-GTC TGC GTC ACC GCC-3′), which contains consensus binding sequences for AP-1 and the CREB/ATF family (Supplemental Tables 2–4), was required for *MIDN* expression. Furthermore, this sequence is conserved among mammals, which suggests universal roles in *MIDN* expression. We found that AP-1 activity, rather than CREB, was involved in *MIDN* expression as demonstrated by attenuation of *MIDN* promoter activity by both a pharmacological inhibitor (SR11302) and decoy ODN for AP-1, whereas the dominant-negative CREB S133A mutant did not decrease its promoter activity (Figs. 7 and 8). Additionally, insulin promoted DNA binding of both c-FOS and c-JUN isoforms to the predicted AP-1 consensus binding sequence (Fig. 8E), which suggested that both AP-1 isoforms are required for *MIDN* expression. AP-1 activity is regulated at multiple levels. For example, expression of AP-1 components is controlled by mRNA synthesis and stability as ERKs strongly stimulate AP-1 activity via de novo synthesis of c-FOS and c-JUN. Additionally, the DNA-binding ability and transactivating capacity of AP-1 are controlled by post-translational modifications, which include phosphorylation and ubiquitination as JUN N-terminal kinase phosphorylates c-JUN. In our study, insulin actually promoted *c-FOS* expression at mRNA and protein levels in an ERK1/2-dependent manner (Fig. 8, A and B), and ERK1/2 was involved in *MIDN* expression induced by insulin (Fig. 3), indicating that the ERK1/2/AP-1 pathways are essential for *MIDN* expression. Because c-FOS protein levels were partially, but significantly, reduced by a PI3-kinase inhibitor (Fig. 8B; Supplemental Fig. 8), AP-1 activity was also regulated by the PI3-kinase pathway via a post-translational modification. Because inhibition of PI3-kinase and ERK1/2 suppressed *MIDN* expression to similar extents (Fig. 3), the PI3-kinase pathway is also required for *MIDN* expression although the downstream signaling pathway is unclear. Both ERK1/2 and PI3-kinase are essential for neuronal differentiation and survival, and targeting these pathways has been proposed as a reasonable approach to suppress various neurodegenerative disorders (Markus et al., 2002; Obara et al., 2004; Rai et al., 2019). MIDN induced through ERK signaling is responsible for neurite outgrowth in PC12 cells (Obara et al., 2017); therefore, MIDN is assumed to be a key regulator in the maintenance of appropriate neuronal functions, and MIDN dysfunction can be a risk factor for the onset and progression of neurodegenerative disorders, such as PD. Therefore, drugs that promote the *MIDN* expression may have potential to be a novel medicine for PD, which may be useful for not only patients who have *MIDN* copy number loss, but also for those who have the normal copy number.

In summary, we demonstrated that insulin promotes *MIDN* expression via ERK1/2 and PI3-kinase pathways. Furthermore, we identified the important region of the *MIDN* promoter and showed that transcription factors, including AP-1, positively regulate *MIDN* expression, whereas TFAP2 negatively regulates basal and insulin-induced *MIDN* expression. Identification of MIDN-binding partners and the clarification of MIDN roles in vivo are key future studies.

Acknowledgments

The authors thank Dr. Satoshi Maegawa (Shiga University of Medical Science, Japan) and Dr. Takeo Saneyoshi (Kyoto University, Japan) for providing the plasmids encoding *TFAP2B* and *CREB* mutant, respectively, Ryoko Murakami, Yuki Miyano, and Dr. Hidenori Sato (Yamagata University School of Medicine, Japan)

for GC-rich DNA sequencing, the JASPAR2020 database (http://jaspar.genereg.net) group members who provided the transcription factor binding profiles, and Jeremy Allen, from Edanz Group (https://jp.edanz.com/ac) for editing a draft of this manuscript.

Authorship Contributions

Participated in research design: Obara, Hosoi, Ishii.

Conducted experiments: Sagehashi, Maruyama, Nakagawa.

Performed data analysis: Sagehashi, Nakagawa.

Wrote or contributed to the writing of the manuscript: Obara, Nakagawa, Ishii.

References

Allen SJ, Watson JJ, Shoemark DK, Barua NU, and Patel NK (2013) GDNF, NGF and BDNF as therapeutic options for neurodegeneration. *Pharmacol Ther* **138**:155–175.

Athauda D, Maclagan K, Budnik N, Zampedri L, Hibbert S, Aviles-Olmos I, Chowdhury K, Skene SS, Limousin P, and Foltynie T (2019) Post hoc analysis of the Exenatide-PD trial-Factors that predict response. *Eur J Neurosci* **49**:410–421.

Athauda D, Maclagan K, Skene SS, Bajwa-Joseph M, Letchford D, Chowdhury K, Hibbert S, Budnik N, Zampedri L, Dickson J, et al. (2017) Exenatide once weekly versus placebo in Parkinson's disease: a randomised, double-blind, placebo-controlled trial. *Lancet* **390**:1664–1675.

Billingsley KJ, Bandres-Ciga S, Ding J, Hernandez D, Gibbs JR, and Blauwendraat C; International Parkinson's Disease Genomics Consortium (IPDGC) (2020) MIDN locus structural variants and Parkinson's Disease risk. *Ann Clin Transl Neurol* **7**:602–603.

Billingsley KJ, Bandres-Ciga S, Saez-Atienzar S, and Singleton AB (2018) Genetic risk factors in Parkinson's disease. *Cell Tissue Res* **373**:9–20.

Blauwendraat C, Nalls MA, and Singleton AB (2020) The genetic architecture of Parkinson's disease. *Lancet Neurol* **19**:170–178.

Butler MG, Rafi SK, Hossain W, Stephan DA, and Manzardo AM (2015) Whole exome sequencing in females with autism implicates novel and candidate genes. *Int J Mol Sci* **16**:1312–1335.

Craft S and Watson GS (2004) Insulin and neurodegenerative disease: shared and specific mechanisms. *Lancet Neurol* **3**:169–178.

Fornes O, Castro-Mondragon JA, Khan A, van der Lee R, Zhang X, Richmond PA, Modi BP, Correard S, Gheorghe M, Baranašić D, et al. (2020) JASPAR 2020: update of the open-access database of transcription factor binding profiles. *Nucleic Acids Res* **48** (D1):D87–D92.

Fuke T, Yoshizaki T, Kondo M, Morino K, Obata T, Ugi S, Nishio Y, Maeda S, Kashiwagi A, and Maegawa H (2010) Transcription factor AP-2beta inhibits expression and secretion of leptin, an insulin-sensitizing hormone, in 3T3-L1 adipocytes. *Int J Obes* **34**:670–678.

Ghasemi R, Haeri A, Dargahi L, Mohamed Z, and Ahmadiani A (2013) Insulin in the brain: sources, localization and functions. *Mol Neurobiol* **47**:145–171.

Giovannone B, Tsiaras WG, de la Monte S, Klysik J, Lautier C, Karashchuk G, Goldwurm S, and Smith RJ (2009) GIGYF2 gene disruption in mice results in neurodegeneration and altered insulin-like growth factor signaling. *Hum Mol Genet* **18**:4629–4639.

Gray SM and Barrett EJ (2018) Insulin transport into the brain. *Am J Physiol Cell Physiol* **315**:C125–C136.

Hofmeister-Brix A, Kollmann K, Langer S, Schultz J, Lenzen S, and Baltrusch S (2013) Identification of the ubiquitin-like domain of midnolin as a new glucokinase interaction partner. *J Biol Chem* **288**:35824–35839.

Honda T, Obara Y, Yamauchi A, Couvillon AD, Mason JJ, Ishii K, and Nakahata N (2015) Phosphorylation of ERK5 on Thr732 is associated with ERK5 nuclear localization and ERK5-dependent transcription. *PLoS One* **10**:e0117914.

Ikram F, Ackermann S, Kahlert Y, Volland R, Roels F, Engesser A, Hertwig F, Kocak H, Hero B, Dreidax D, et al. (2016) Transcription factor activating protein 2 beta (TFAP2B) mediates noradrenergic neuronal differentiation in neuroblastoma. *Mol Oncol* **10**:344–359.

Kashino Y, Obara Y, Okamoto Y, Saneyoshi T, Hayashi Y, and Ishii K (2018) ERK5 Phosphorylates K_v4.2 and Inhibits Inactivation of the A-Type Current in PC12 Cells. *Int J Mol Sci* **19**:7.

Lautier C, Goldwurm S, Dürr A, Giovannone B, Tsiaras WG, Pezzoli G, Brice A, and Smith RJ (2008) Mutations in the GIGYF2 (TNRC15) gene at the PARK11 locus in familial Parkinson disease. *Am J Hum Genet* **82**:822–833.

Li JJ, Westergaard C, Ghosh P, and Colburn NH (1997) Inhibitors of both nuclear factor-kappaB and activator protein-1 activation block the neoplastic transformation response. *Cancer Res* **57**:3569–3576.

Lill CM (2016) Genetics of Parkinson's disease. *Mol Cell Probes* **30**:386–396.

Markus A, Patel TD, and Snider WD (2002) Neurotrophic factors and axonal growth. *Curr Opin Neurobiol* **12**:523–531.

Molnár G, Faragó N, Kocsis AK, Rózsa M, Lovas S, Boldog E, Báldi R, Csajbók É, Gardi J, Puskás LG, et al. (2014) GABAergic neurogliaform cells represent local sources of insulin in the cerebral cortex. *J Neurosci* **34**:1133–1137.

Moriyama I, Ishihara S, Rumi MAK, Aziz MDM, Mishima Y, Oshima N, Kadota C, Kadowaki Y, Amano Y, and Kinoshita Y (2008) Decoy oligodeoxynucleotide targeting activator protein-1 (AP-1) attenuates intestinal inflammation in murine experimental colitis. *Lab Invest* **88**:652–663.

Moroo I, Yamada T, Makino H, Tooyama I, McGeer PL, McGeer EG, and Hirayama K (1994) Loss of insulin receptor immunoreactivity from the substantia nigra pars compacta neurons in Parkinson's disease. *Acta Neuropathol* **87**:343–348.

Nakagawa T, Hattori S, Nobuta R, Kimura R, Nakagawa M, Matsumoto M, Nagasawa Y, Funayama R, Miyakawa T, Inada T, et al. (2020) The autism-related protein SETD5 controls neural cell proliferation through epigenetic regulation of rDNA expression. *iScience* **23**:101030.

Nemoto T, Toyoshima-Aoyama F, Yanagita T, Maruta T, Fujita H, Koshida T, Yonaha T, Wada A, Sawaguchi A, and Murakami M (2014) New insights concerning insulin synthesis and its secretion in rat hippocampus and cerebral cortex: amyloid-β1-42-induced reduction of proinsulin level via glycogen synthase kinase-3β. *Cell Signal* **26**:253–259.

Novak P, Pimentel Maldonado DA, and Novak V (2019) Safety and preliminary efficacy of intranasal insulin for cognitive impairment in Parkinson disease and multiple system atrophy: A double-blinded placebo-controlled pilot study. *PLoS One* **14**:e0214364.

Obara Y, Imai T, Sato H, Takeda Y, Kato T, and Ishii K (2017) Midnolin is a novel regulator of parkin expression and is associated with Parkinson's Disease. *Sci Rep* **7**:5885.

Obara Y and Ishii K (2018) Transcriptome Analysis Reveals That Midnolin Regulates mRNA Expression Levels of Multiple Parkinson's Disease Causative Genes. *Biol Pharm Bull* **41**:20–23.

Obara Y, Labudda K, Dillon TJ, and Stork PJ (2004) PKA phosphorylation of Src mediates Rap1 activation in NGF and cAMP signaling in PC12 cells. *J Cell Sci* **117**:6085–6094.

Obara Y, Sato H, Nakayama T, Kato T, and Ishii K (2019) Midnolin is a confirmed genetic risk factor for Parkinson's disease. *Ann Clin Transl Neurol* **6**:2205–2211.

Obara Y, Sato H, Nakayama T, Kato T, and Ishii K (2020) Reply to: MIDN locus structural variants and Parkinson's disease risk. *Ann Clin Transl Neurol* **7**:604–605.

Rai SN, Dilnashin H, Birla H, Singh SS, Zahra W, Rathore AS, Singh BK, and Singh SP (2019) The Role of PI3K/Akt and ERK in Neurodegenerative Disorders. *Neurotox Res* **35**:775–795.

Sakane C and Shidoji Y (2011) Reversible upregulation of tropomyosin-related kinase receptor B by geranylgeranoic acid in human neuroblastoma SH-SY5Y cells. *J Neurooncol* **104**:705–713.

Sánchez-Gómez A, Alcarraz-Vizán G, Fernández M, Fernández-Santiago R, Ezquerra M, Cámara A, Serrano M, Novials A, Muñoz E, Valldeoriola F, et al. (2020) Peripheral insulin and amylin levels in Parkinson's disease. *Parkinsonism Relat Disord* **79**:91–96.

Sánchez-Gómez A, Compta Y, and Martí MJ (2021) Insulin-releasing or insulin-sensitizing drugs in Parkinson's disease? Choosing a pathway. *Parkinsonism Relat Disord* **93**:109–110.

Scott L, Dawson VL, and Dawson TM (2017) Trumping neurodegeneration: Targeting common pathways regulated by autosomal recessive Parkinson's disease genes. *Exp Neurol* **298** (Pt B):191–201.

Shaughness M, Acs D, Brabazon F, Hockenbury N and Byrnes KR (2020) Role of Insulin in Neurotrauma and Neurodegeneration: A Review. *Front Neurosci-Switz* **14**.

Shiohira H, Kitaoka A, Enjoji M, Uno T, and Nakashima M (2012) Am80 induces neuronal differentiation via increased tropomyosin-related kinase B expression in a human neuroblastoma SH-SY5Y cell line. *Biomed Res* **33**:291–297.

Singh V, Bala R, Chakraborty A, Rajender S, Trivedi S, and Singh K (2019) Duplications in 19p13.3 are associated with male infertility. *J Assist Reprod Genet* **36**:2171–2179.

Smolders S and Van Broeckhoven C (2020) Genetic perspective on the synergistic connection between vesicular transport, lysosomal and mitochondrial pathways associated with Parkinson's disease pathogenesis. *Acta Neuropathol Commun* **8**:63.

Trejo JL, Carro E, Garcia-Galloway E, and Torres-Aleman I (2004) Role of insulin-like growth factor I signaling in neurodegenerative diseases. *J Mol Med (Berl)* **82**:156–162.

Tsukahara M, Suemori H, Noguchi S, Ji ZS, and Tsunoo H (2000) Novel nucleolar protein, midnolin, is expressed in the mesencephalon during mouse development. *Gene* **254**:45–55.

Wada A, Yokoo H, Yanagita T, and Kobayashi H (2005) New twist on neuronal insulin receptor signaling in health, disease, and therapeutics. *J Pharmacol Sci* **99**:128–143.

York RD, Yao H, Dillon T, Ellig CL, Eckert SP, McCleskey EW, and Stork PJ (1998) Rap1 mediates sustained MAP kinase activation induced by nerve growth factor. *Nature* **392**:622–626.

Zhao WQ and Alkon DL (2001) Role of insulin and insulin receptor in learning and memory. *Mol Cell Endocrinol* **177**:125–134.

Address correspondence to: Dr. Yutaro Obara, Department of Pharmacology, Yamagata University School of Medicine, Iida-Nishi 2-2-2, Yamagata 990-9585, Japan. E-mail: obaray@med.id.yamagata-u.ac.jp

The Journal of Pharmacology and Experimental Therapeutics
(JPET-AR-2021-001076)

Supplemental Materials

Insulin enhances gene expression of *Midnolin*, a novel genetic risk factor for Parkinson's disease, via ERK, PI3-kinase and multiple transcription factors in SH-SY5Y cells

Naoki Sagehashi[1], Yutaro Obara[1,*], Ohki Maruyama[1], Tadashi Nakagawa[2], Toru Hosoi[2], Kuniaki Ishii[1]

[1]*Department of Pharmacology, Yamagata University School of Medicine, Iida-Nishi 2-2-2, Yamagata 990-9585, Japan*

[2]*Department of Clinical Pharmacology, Faculty of Pharmaceutical Sciences, Sanyo-Onoda City University, Daigaku-Dori 1-1-1, Sanyo Onoda, 756-0884, Japan*.

***Corresponding author:** Yutaro Obara, Ph.D.

Department of Pharmacology, Yamagata University School of Medicine, Iida-Nishi 2-2-2, Yamagata 990-9585, Japan.

Phone: +81-23-628-5233; FAX: +81-23-628-5235; E-mail: obaray@med.id.yamagata-u.ac.jp

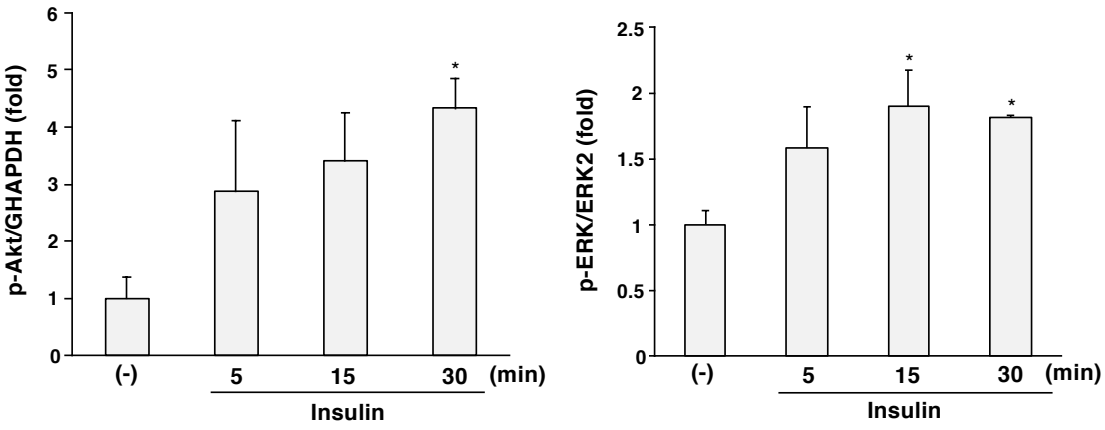

Supplementary Figure S1: SH-SY5Y cells were stimulated with insulin (1 μM) for 5, 15, and 30 min. Phosphorylation of Akt and ERK1/2 was examined by Western blotting and relative band intensities were analysed. Phosphorylation of Akt and ERK1/2 was significantly promoted by insulin (n=3, $^{*}p<0.05$).

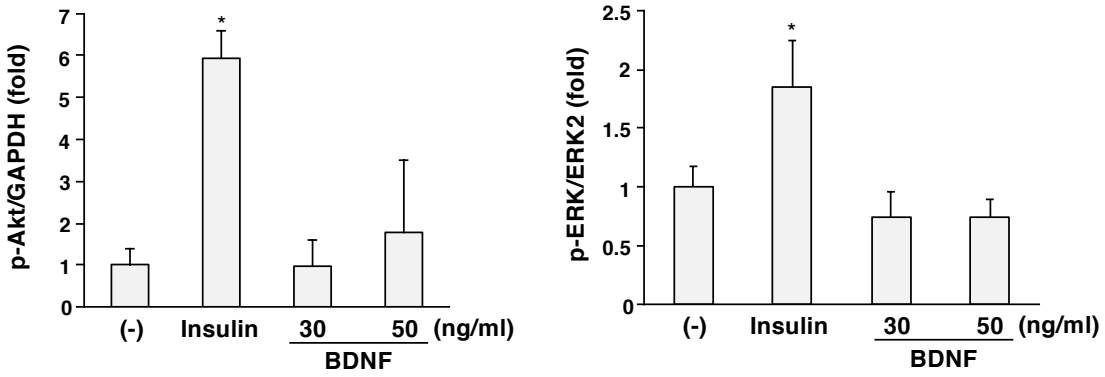

Supplementary Figure S2: SH-SY5Y cells were stimulated with insulin (1 μM) or BDNF (30 or 50 ng/ml) for 5 min. Phosphorylation of Akt and ERK1/2 was examined by Western blotting and relative band intensities were analysed. Phosphorylation of Akt and ERK1/2 was significantly promoted by insulin, not BDNF (n=3, $^{*}p<0.05$).

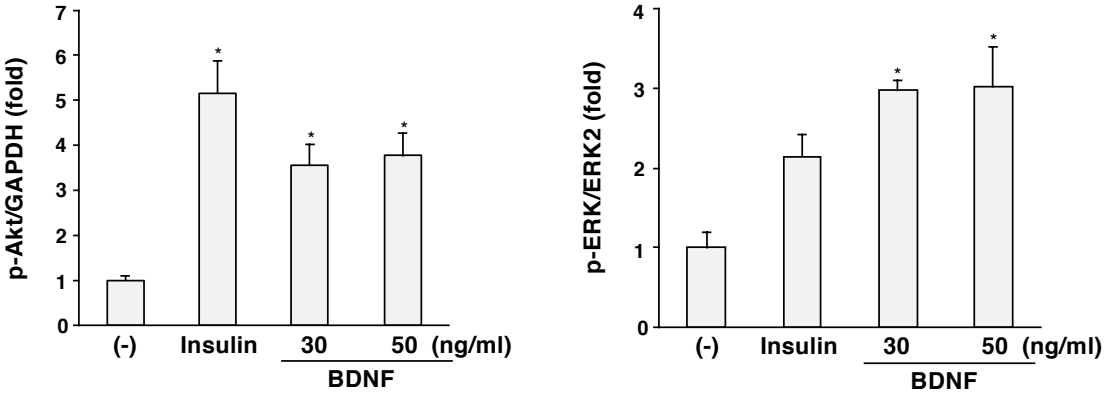

Supplementary Figure S3: SH-SY5Y cells were incubated in the presence of all-trans retinoic acid (10 μM) for 5 days, and stimulated with insulin (1 μM) or BDNF (30 or 50 ng/ml) for 5 min. Phosphorylation of Akt and ERK1/2 was examined by Western blotting and relative band intensities were analysed. Phosphorylation of Akt and ERK1/2 was significantly promoted by BDNF (30 or 50 ng/ml) (n=3, $^{*}p<0.05$).

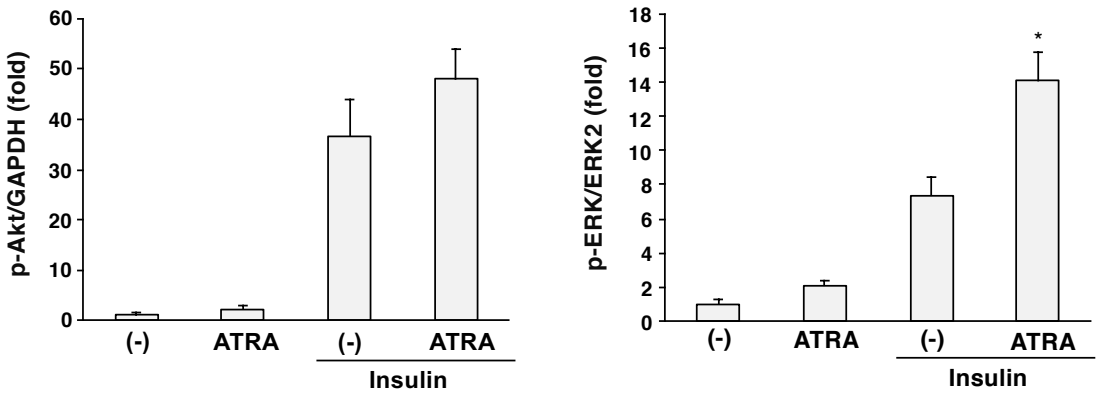

Supplementary Figure S4: SH-SY5Y cells were incubated in the presence or absence of all-trans retinoic acid (ATRA) (10 μM) for 5 days, and stimulated with insulin (1 μM) for 5 min. Phosphorylation of Akt and ERK1/2 was examined by Western blotting and relative band intensities were analysed. Phosphorylation of ERK1/2 by insulin was significantly promoted by ATRA (n=3, $^{*}p<0.05$).

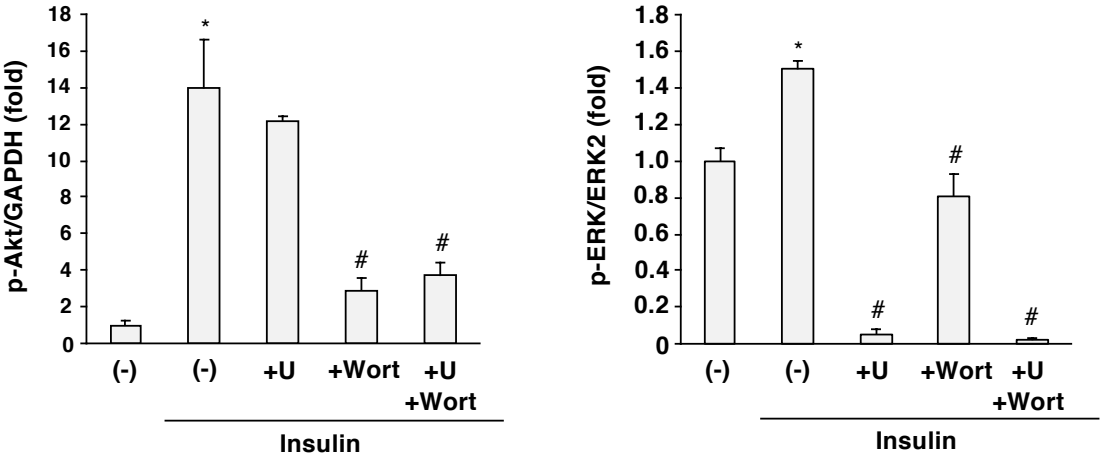

Supplementary Figure S5: SH-SY5Y cells were pre-incubated with or without U0126 (U, 30 μM) or wortmannin (Wort, 500 nM) for 30 min, then stimulated with insulin (1 μM) for 2 h. Phosphorylation of Akt and ERK1/2 was examined by Western blotting and relative band intensities were analysed. Phosphorylation of Akt was promoted by insulin (n=3, $^{*}p<0.05$), which was significantly blocked by wortmannin and combination of wortmannin and U0126 (n=3, $^{\#}p<0.05$). Phosphorylation of ERK1/2 was promoted by insulin (n=3, $^{*}p<0.05$), which was significantly blocked by U0126, wortmannin and combination of wortmannin and U0126 (n=3, $^{\#}p<0.05$).

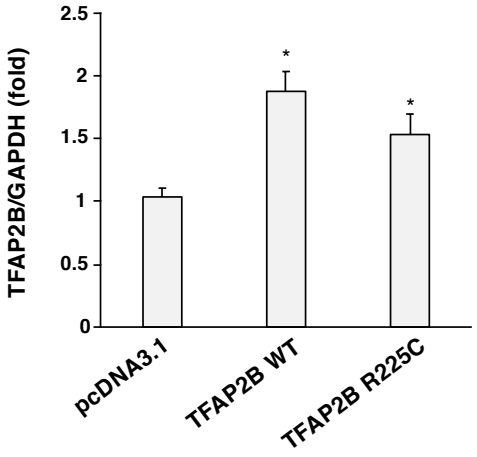

Supplementary Figure S6: SH-SY5Y cells were co-transfected with wild-type *MIDN* promoter (-150~+125 bp) linked to *luciferase* in a promoter-less plasmid (pGL3) and empty vector (pcDNA3.1), wild-type TFAP2B (WT) or a dominant-negative TFAP2B mutant (R225C). Overexpression of TFAP2B and TFAP2B-R225C was examined by Western blotting and relative band intensities were analysed. TFAP2B expression levels were significantly increased by transfection with TFAP2 WT or R225C mutants (n=3, $^{*}p<0.05$).

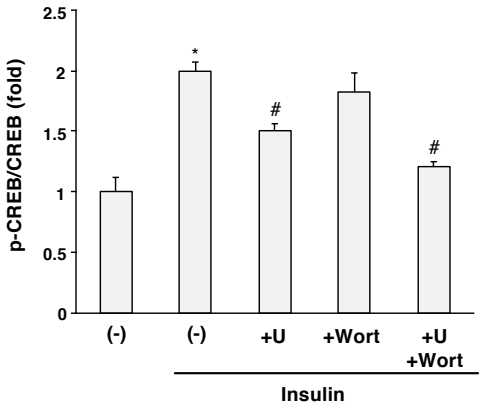

Supplementary Figure S7: SH-SY5Y cells were preincubated in the presence or absence of U0126 (U, 30 μM) or wortmannin (Wort, 500 nM) for 30 min and then stimulated with insulin (1 μM) for 2 h. Phosphorylation of CREB at Ser133 was examined by Western blotting and relative band intensities were analysed. Insulin significantly promoted CREB phosphorylation (n=3, $*p<0.05$), which was inhibited by U0126 and the combination of U0126 and wortmannin (n=3, $^{\#}p<0.05$).

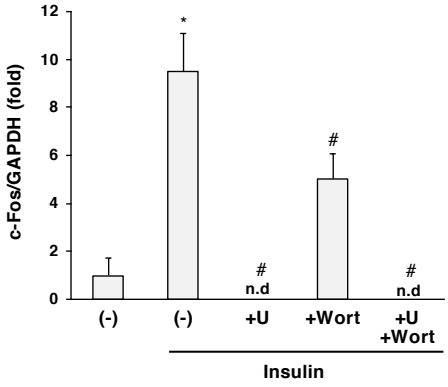

Supplementary Figure S8: SH-SY5Y cells were preincubated in the presence or absence of U0126 (U, 30 μM) or wortmannin (Wort, 500 nM) for 30 min and then stimulated with insulin (1 μM) for 2 h. c-FOS expression was examined by Western blotting and relative band intensities were analysed. Insulin significantly promoted c-FOS protein expression (n=3, $*p<0.05$), which was inhibited by U0126, wortmannin, and combination of U0126 and wortmannin (n=3, $^{\#}p<0.05$).

Matrix ID	Name	Score	Relative score	Start	End	Strand	Predicted sequence
MA0810.1	TFAP2A(var.2)	12.9646	0.954179721	12	23	+	CGCCCCAGGGCC
MA0524.1	TFAP2C	12.6803	0.92347673	9	23	+	AGGCGCCCCAGGGCC
MA0524.2	TFAP2C	12.291	0.933909139	12	23	+	CGCCCCAGGGCC
MA0814.2	TFAP2C(var.2)	12.2551	0.897942187	10	23	-	GGCCCTGGGGCGCC
MA0811.1	TFAP2B	12.2031	0.933887188	12	23	+	CGCCCCAGGGCC
MA0003.2	TFAP2A	12.0335	0.886064059	9	23	+	AGGCGCCCCAGGGCC
MA0811.1	TFAP2B	11.282	0.919278026	12	23	-	GGCCCTGGGGCG
MA1569.1	TFAP2E	11.2661	0.952010793	12	22	+	CGCCCCAGGGC
MA1569.1	TFAP2E	11.0593	0.949249415	12	22	-	GCCCTGGGGCG
MA0524.2	TFAP2C	10.8386	0.910307731	12	23	-	GGCCCTGGGGCG
MA0810.1	TFAP2A(var.2)	10.8059	0.920674597	12	23	-	GGCCCTGGGGCG
MA0003.3	TFAP2A	10.5649	0.920878931	12	22	+	CGCCCCAGGGC
MA0003.4	TFAP2A	10.2957	0.859193137	10	23	+	GGCGCCCCAGGGCC
MA0003.1	TFAP2A	10.0665	0.989385105	14	22	-	GCCCTGGGG
MA0003.1	TFAP2A	10.0297	0.98818336	13	21	+	GCCCCAGGG
MA0813.1	TFAP2B(var.3)	9.36804	0.859461323	1	13	+	AGCCGTCAAGGCG
MA0872.1	TFAP2A(var.3)	9.06176	0.849320252	1	13	+	AGCCGTCAAGGCG
MA0812.1	TFAP2B(var.2)	8.98191	0.886348154	12	22	+	CGCCCCAGGGC
MA0813.1	TFAP2B(var.3)	8.8645	0.851962608	1	13	-	CGCCTTGACGGCT
MA0815.1	TFAP2C(var.3)	8.82907	0.858807495	1	13	+	AGCCGTCAAGGCG
MA0815.1	TFAP2C(var.3)	8.58279	0.855394067	1	13	-	CGCCTTGACGGCT
MA0814.1	TFAP2C(var.2)	8.21686	0.8796537	12	22	+	CGCCCCAGGGC
MA0872.1	TFAP2A(var.3)	7.82864	0.830381906	1	13	-	CGCCTTGACGGCT
MA0814.1	TFAP2C(var.2)	7.46944	0.867666673	12	22	-	GCCCTGGGGCG
MA0003.3	TFAP2A	6.95694	0.864161308	12	22	-	GCCCTGGGGCG
MA0812.1	TFAP2B(var.2)	6.88858	0.854612353	12	22	-	GCCCTGGGGCG
MA1569.1	TFAP2E	6.5672	0.889266628	13	23	+	GCCCCAGGGCC
MA1569.1	TFAP2E	6.41803	0.887274736	13	23	-	GGCCCTGGGGC
MA0003.1	TFAP2A	5.87727	0.852680514	4	12	-	GCCTTGACG
MA0003.1	TFAP2A	5.51403	0.840827035	2	10	+	GCCGTCAAG
MA0003.3	TFAP2A	3.96691	0.817158131	13	23	+	GCCCCAGGGCC

Supplementary Table S1: *In silico* JASPAR database analysis. TFAP2 family members that putatively bind to the *MIDN* promoter region (-121 bp to -99 bp: 5′ -AGC CGT CAA GGC GCC CCA GGG CC-3′) are shown with scores and predicted sequences. Relative profile score threshold was 80%.

Matrix ID	Name	Score	Relative score	Start	End	Strand	Predicted sequence
MA1128.1	FOSL1::JUN	10.5189	0.888102383	1	13	-	CGGTGACGCAGAC
MA1141.1	FOS::JUND	10.1338	0.876127251	1	13	+	GTCTGCGTCACCG
MA1130.1	FOSL2::JUN	10.0364	0.887397998	1	12	+	GTCTGCGTCACC
MA0605.1	Atf3	10.0341	0.917590904	5	12	-	GGTGACGC
MA0099.3	FOS::JUN	9.85091	0.888647329	3	12	+	CTGCGTCACC
MA1137.1	FOSL1::JUNB	9.82596	0.872382981	1	13	-	CGGTGACGCAGAC
MA1144.1	FOSL2::JUND	8.85723	0.870163853	3	12	-	GGTGACGCAG
MA1142.1	FOSL1::JUND	8.71236	0.881633579	3	12	-	GGTGACGCAG
MA1135.1	FOSB::JUNB	8.42115	0.865478321	3	12	-	GGTGACGCAG
MA1134.1	FOS::JUNB	7.81613	0.844404127	2	13	+	TCTGCGTCACCG
MA0099.2	FOS::JUN	7.79437	0.895254664	4	10	-	TGACGCA
MA1138.1	FOSL2::JUNB	7.68241	0.851448171	3	12	-	GGTGACGCAG
MA1143.1	FOSL1::JUND(var.2)	7.49865	0.830699773	2	11	-	GTGACGCAGA
MA0477.1	FOSL1	7.21865	0.868823434	2	12	-	GGTGACGCAGA
MA0099.1	JUN::FOS	7.20198	0.84893485	4	11	-	GTGACGCA
MA0478.1	FOSL2	6.825	0.867514027	3	13	-	CGGTGACGCAG
MA0099.1	JUN::FOS	6.48991	0.82535644	3	10	+	CTGCGTCA
MA0477.2	FOSL1	5.92422	0.815666967	1	13	-	CGGTGACGCAGAC
MA0099.2	FOS::JUN	5.52117	0.812279091	4	10	+	TGCGTCA
MA0476.1	FOS	3.91938	0.841211694	2	12	+	TCTGCGTCACC
MA0476.1	FOS	1.21657	0.805163909	2	12	-	GGTGACGCAGA

Supplementary Table S2: *In silico* JASPAR database analysis. FOS family members that putatively bind to the *MIDN* promoter region (-71 bp to -57 bp: 5′ -GTC TGC GTC ACC GCC-3′) are shown with scores and predicted sequences. Relative profile score threshold was 80%.

Matrix ID	Name	Score	Relative score	Start	End	Strand	Predicted sequence
MA1128.1	FOSL1::JUN	10.5189	0.888102383	1	13	-	CGGTGACGCAGAC
MA1141.1	FOS::JUND	10.1338	0.876127251	1	13	+	GTCTGCGTCACCG
MA1130.1	FOSL2::JUN	10.0364	0.887397998	1	12	+	GTCTGCGTCACC
MA0099.3	FOS::JUN	9.85091	0.888647329	3	12	+	CTGCGTCACC
MA1137.1	FOSL1::JUNB	9.82596	0.872382981	1	13	-	CGGTGACGCAGAC
MA1132.1	JUN::JUNB	9.58854	0.883150386	3	12	-	GGTGACGCAG
MA1144.1	FOSL2::JUND	8.85723	0.870163853	3	12	-	GGTGACGCAG
MA1142.1	FOSL1::JUND	8.71236	0.881633579	3	12	-	GGTGACGCAG
MA1135.1	FOSB::JUNB	8.42115	0.865478321	3	12	-	GGTGACGCAG
MA1134.1	FOS::JUNB	7.81613	0.844404127	2	13	+	TCTGCGTCACCG
MA0099.2	FOS::JUN	7.79437	0.895254664	4	10	-	TGACGCA
MA1138.1	FOSL2::JUNB	7.68241	0.851448171	3	12	-	GGTGACGCAG
MA1143.1	FOSL1::JUND(var.2)	7.49865	0.830699773	2	11	-	GTGACGCAGA
MA0099.1	JUN::FOS	7.20198	0.84893485	4	11	-	GTGACGCA
MA0462.2	BATF::JUN	6.76692	0.820083579	2	12	-	GGTGACGCAGA
MA0099.1	JUN::FOS	6.48991	0.82535644	3	10	+	CTGCGTCA
MA0490.1	JUNB	6.10452	0.868813616	3	13	-	CGGTGACGCAG
MA0089.1	MAFG::NFE2L1	5.91912	0.874700179	7	12	-	GGTGAC
MA0099.2	FOS::JUN	5.52117	0.812279091	4	10	+	TGCGTCA
MA0491.1	JUND	2.17727	0.836314736	2	12	-	GGTGACGCAGA
MA0491.1	JUND	1.84511	0.832621369	2	12	+	TCTGCGTCACC

Supplementary Table S3: *In silico* JASPAR database analysis. JUN family members that putatively bind to the *MIDN* promoter region (-71 bp to -57 bp: 5′ -GTC TGC GTC ACC GCC-3′) are shown with scores and predicted sequences. Relative profile score threshold was 80%.

Matrix ID	Name	Score	Relative score	Start	End	Strand	Predicted sequence
MA0018.1	CREB1	11.1485	0.925408212	4	15	-	GGCGGTGACGCA
MA0604.1	Atf1	10.9754	0.955559593	4	11	-	GTGACGCA
MA1474.1	CREB3L4	6.80677	0.802448842	1	12	+	GTCTGCGTCACC
MA0018.2	CREB1	6.62373	0.818912614	3	10	-	TGACGCAG

Supplementary Table S4: *In silico* JASPAR database analysis. CREB/ATF family members that putatively bind to the *MIDN* promoter region (-71 bp to -57 bp: 5′ -GTC TGC GTC ACC GCC-3′) are shown with scores and predicted sequences. Relative profile score threshold was 80%.